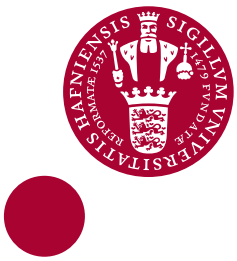

The influence of climate on early and burial diagenesis of Triassic and Jurassic sandstones from the Norwegian–Danish Basin

Weibel, Rikke ; Olivarius, Mette; Kjoller, Claus; Kristensen, Lars; Hjuler, Morten Leth; Friis, Henrik; Pedersen, Per Kent; Boyce, Adrian; Andersen, Morten Sparre; Kamla, Elina; Boldreel, Lars Ole; Mathiesen, Anders; Nielsen, Lars Henrik

Published in:
The Depositional Record

DOI:
10.1002/dep2.27

Publication date:
2017

Document version
Publisher's PDF, also known as Version of record

Citation for published version (APA):
Weibel, R., Olivarius, M., Kjoller, C., Kristensen, L., Hjuler, M. L., Friis, H., Pedersen, P. K., Boyce, A., Andersen, M. S., Kamla, E., Boldreel, L. O., Mathiesen, A., & Nielsen, L. H. (2017). The influence of climate on early and burial diagenesis of Triassic and Jurassic sandstones from the Norwegian–Danish Basin. *The Depositional Record*, *3*(1), 60-91. https://doi.org/10.1002/dep2.27

The Depositional Record
The journal of the International Association of Sedimentologists
Open Access

ORIGINAL RESEARCH ARTICLE

The influence of climate on early and burial diagenesis of Triassic and Jurassic sandstones from the Norwegian–Danish Basin

RIKKE WEIBEL*, METTE OLIVARIUS*,†, CLAUS KJØLLER*, LARS KRISTENSEN*, MORTEN LETH HJULER*, HENRIK FRIIS†, PER KENT PEDERSEN‡, ADRIAN BOYCE§, MORTEN SPARRE ANDERSEN*, ELINA KAMLA*, LARS OLE BOLDREEL¶, ANDERS MATHIESEN* and LARS HENRIK NIELSEN*

*GEUS, Geological Survey of Denmark and Greenland, Øster Voldgade 10, 1350 Copenhagen K, Denmark E-mail: rwh@geus.dk
†Department of Geosciences, University of Aarhus, Høegh-Guldbergs Gade 2, 8000 Århus C, Denmark
‡Department of Geoscience, University of Calgary, 2500 University Drive NW, Calgary, T2N 1N4, Canada
§SUERC, Scottish Universities Environmental Research Centre, Rankine Avenue, East Kilbride, G75 0QF, UK
¶Department of Geosciences and Natural Resource Management, University of Copenhagen, 1350 Copenhagen K, Denmark

Keywords
Carbonate cement, clay minerals, climate, detrital composition/maturity of detritus, Fe-rich phases, palaeohydrology, sandstone diagenesis.

Manuscript received: 13 January 2017; Accepted: 23 May 2017

The Depositional Record 2017; 3(1): 60–91

doi: 10.1002/dep2.27

ABSTRACT

Climate changes preserved in sandstones are documented by comparing the sediment composition and early diagenetic changes in sandstones deposited during arid to semi-arid conditions, the Skagerrak Formation, with sandstones of the Gassum Formation deposited in a humid well-vegetated environment. The study area covers the easternmost part of the Norwegian–Danish Basin, for which the Fennoscandian Shield functioned as sediment source area. The depositional environments of the formations, their distribution and burial depths are well-constrained, facilitating a comprehensive petrographical and geochemical study complemented by porosity and permeability measurements of cores widely distributed in the basin (1700 to 5900 m burial depth). The Skagerrak Formation had an immature composition with more abundant feldspar, rock fragments and a larger variability in the heavy mineral assemblage when compared to the Gassum Formation, which was characterized by quartz and more stable heavy minerals. The arid to semi-arid climate led to early oxidizing conditions under which abundant iron-oxide/hydroxide coatings formed, while the evaporative processes occasionally resulted in caliche and gypsum precipitation. Under the humid climate, kaolinite precipitated due to leaching of feldspar and mica, and the abundant organic matter caused reducing conditions, which led to other Fe-rich phases, i.e. pyrite, Fe-chlorite and siderite. The inherited early diagenetic pore fluids and mineral assemblage also affect the mineral changes occurring during deeper burial, so dolomite preferentially formed in the sandstones deposited in an arid environment, while ankerite characterizes sandstones deposited under humid conditions. In addition to climate-induced burial diagenetic changes, there are also temperature-dependent phases, such as illite and quartz cement. Despite the same sediment source area remaining active during the entire period, the sediments that reached the Norwegian–Danish Basin were immature during the arid interval, although mature during the humid period. This has implications for provenance investigations as well as diagenetic investigations of sandstone reservoir quality.

INTRODUCTION

Climate conditions, such as temperature and precipitation intensity, and geomorphology of the sediment source area define the intensity of weathering in the sediment source area, as well as the composition of the weathering products (Parrish *et al.*, 1993; Jeans *et al.*, 2001). Towards the end of the Triassic period, the prevailing arid to semi-arid climate became more humid (Manspeizer, 1994; Veevers, 1994; Ahlberg *et al.*, 2002; Francis, 2009). In the Norwegian–Danish Basin, these changes in climate are reflected by a shift from the reddish alluvial and fluvial deposits of the Triassic Skagerrak Formation to the greyish paralic and marine deposits of the Upper Triassic–Lower Jurassic Gassum Formation.

Besides determining the composition of the material supplied to the basin, the climate controls the water availability and geochemical conditions in the post-depositional environment. The low precipitation in an arid climate leads to overall oxidizing conditions where evaporation plays an important role during early diagenesis. Rare organic matter gives rise to reduction spots with locally different early diagenetic alterations (Ixer *et al.*, 1979; Burley, 1984; Surdam *et al.*, 1993; Weibel, 1998; Weibel & Friis, 2004). Iron-containing minerals in particular are affected by the different redox conditions resulting in dissimilar alteration products (Weibel, 1998; Weibel & Friis, 2004, 2007). During Late Triassic–Early Jurassic times, a humid climate with abundant and diverse plant life due to the higher precipitation led to more intense meteoric water flushing of the sediments. Organic matter dispersed in the sediments, combined with occasional coal beds, created reducing early diagenetic conditions. As the detrital clays supplied to the basin vary according to climate, so do the authigenic clays in the sandstones. Kaolinite and mica are abundant in sandstones deposited under humid conditions (Bjørlykke & Aagaard, 1992). In contrast, sandstones deposited under arid conditions have a more diverse clay mineral assemblage, dominated by smectite and chlorite (Burley, 1984; Bjørlykke & Aagaard, 1992; Weibel, 1999).

Previous studies have treated diagenesis in the Skagerrak Formation and the Gassum Formation in the Norwegian–Danish Basin separately without comparing their different diagenetic alterations (Friis, 1987; Weibel, 1998). However, these sediments provide a unique possibility for comparing and contrasting diagenetic developments in sandstones deposited under humid and arid conditions, as it has been documented that the same source area supplied sediment to the basin under the different climates affecting deposition of the Skagerrak and Gassum formations (Larsen, 1966; Larsen & Friis, 1975; Olivarius, 2015; Olivarius & Nielsen, 2016).

The stratigraphic and sedimentological framework of the study area is well-constrained by previous studies (Pedersen & Andersen, 1980; Olsen, 1988; Pedersen, 1998; Nielsen, 2003). The data set comprises cores from the Norwegian–Danish Basin, which allow the effects of both early and deep burial diagenesis to be investigated. The present-day burial depth varies from 900 to 5100 m, which corresponds to estimated maximum burial depths of 1600 to 5700 m when corrected for Neogene uplift (Japsen & Bidstrup, 1999; Japsen *et al.*, 2007). Furthermore, the studied diagenetic alterations were not affected by overpressure or hydrocarbon migration (Thomsen *et al.*, 1987).

The Skagerrak and Gassum formations are used as proxies for arid to semi-arid and humid climate, respectively, and hence represent different palaeohydrological and early diagenetic conditions. Furthermore, the Danish part of the Norwegian–Danish Basin provides the perfect opportunity to (i) compare how different climates affect early diagenesis in fluvial braided stream deposits; (ii) compare early diagenetic processes in various depositional environments (lagoonal, shoreface, fluvio-estuarine, fluvial, alluvial fan, aeolian); (iii) evaluate to what degree later diagenesis is controlled by the early diagenetic pathways defined by climate and depositional conditions; and (iv) evaluate how porosity and permeability are influenced by early diagenetic pathways. This study has implications for provenance investigations, as climate change results in a concomitant change in the mineralogical composition of the sediment being supplied to the basin, which could be falsely interpreted as 'unroofing' in the sediment source area. The consistent provenance of the Triassic and Jurassic sandstones in this part of the Norwegian–Danish Basin ensures that the mineralogically and petrologially differences can be ascribed to climatic and palaeohydrological influence of the early diagenetic regime. Additionally, it has implications for burial diagenetic alterations and reservoir predictions, as this study shows clear differences between sandstones deposited in arid to semi-arid and humid climate.

GEOLOGICAL SETTING AND PALAEOCLIMATE

The Norwegian–Danish Basin formed during Late Carboniferous–Early Permian rifting (Vejbæk, 1997). The basin is limited towards the south by the Ringkøbing–Fyn High and towards the north-east by the Fennoscandian Border Zone, which comprises the Skagerrak–Kattegat Platform and the Sorgenfrei–Tornquist Zone (Fig. 1). The Skagerrak–Kattegat Platform is a large stable platform area, where Mesozoic sediments onlap Precambrian crystalline basement and Palaeozoic successions (Fig. 2).

The Sorgenfrei–Tornquist fault lineament demarcates the stable Fennoscandian Shield and represents the northwestern segment of the Tornquist–Teisseyre Zone (Liboriussen *et al.*, 1987; Mogensen, 1996; Michelsen, 1997). Thick deposits accumulated during Triassic and Jurassic times as the accommodation space increased during thermally controlled subsidence in the post-rift phase. Deepening of the basin away from the Ringkøbing–Fyn High and the Skagerrak–Kattegat Platform is documented by thinning of the Zechstein – Lower and Upper Jurassic – Lower Cretaceous successions on these structural highs (Vejbæk, 1997). Uplift of the Fennoscadian Shield during the beginning of the Mesozoic resulted in erosion of the Fennoscandian basement and its Palaeozoic cover, which supplied the vast majority of the clastic material delivered to the Norwegian–Danish Basin (Zeck *et al.*, 1988).

Depositional environment of the Skagerrak Formation

The Skagerrak Formation comprises red, brown and grey conglomeratic sandstones, mudstones and shales deposited on alluvial fans along the Fennoscandian Border Zone (Deegan & Scull, 1977; Bertelsen, 1980). The thickness of the formation locally exceeds 3000 m according to seismic interpretations. The alluvial fan deposits pass into braided river facies towards the west and south-west (Pedersen & Andersen, 1980; Olsen, 1988). The braided stream facies association consists of greyish red to pale reddish brown fine- to medium-grained sandstones with large-scale cross-bedding, fine-grained parallel lamination or small-scale cross-bedding (Pedersen & Andersen, 1980). The presence of intra-formational mudclasts, either along foresets or as basal lags, is interpreted as alternating

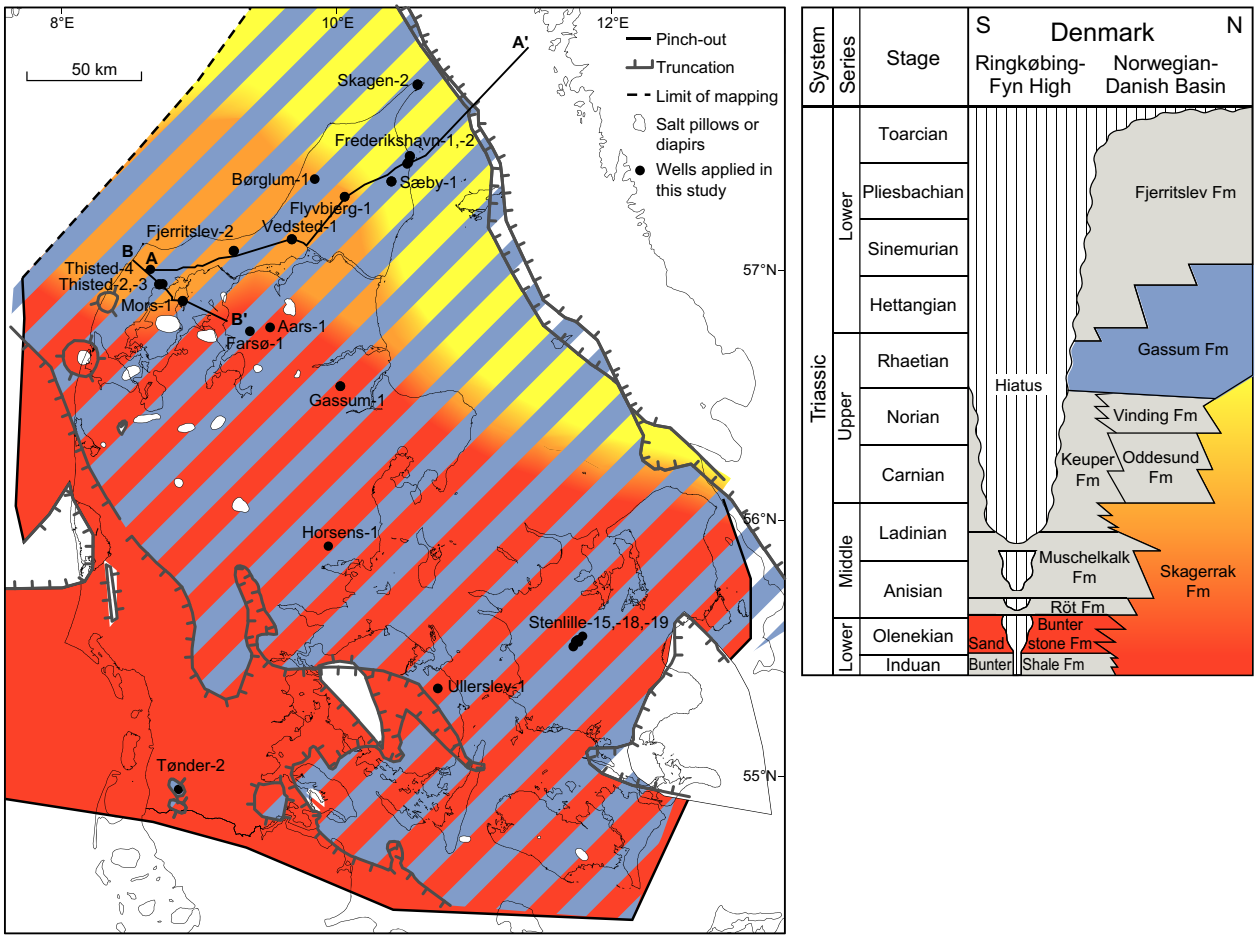

Fig. 1. (A) Map of the Danish Basin, the easternmost part of the Norwegian–Danish Basin, showing the extent of the Skagerrak Formation in reddish-yellow colours and the extent of the Gassum Formation in blue. White areas represent area of no deposition or erosion, due to structural highs and some due to local salt tectonics. Lines mark the surface traces of the seismic profiles. Structural elements modified after Vejbæk (1997). RFH = Ringkøbing–Fyn High. (B) Stratigraphic scheme modified after Michelsen and Clausen (2002) and Nielsen (2003).

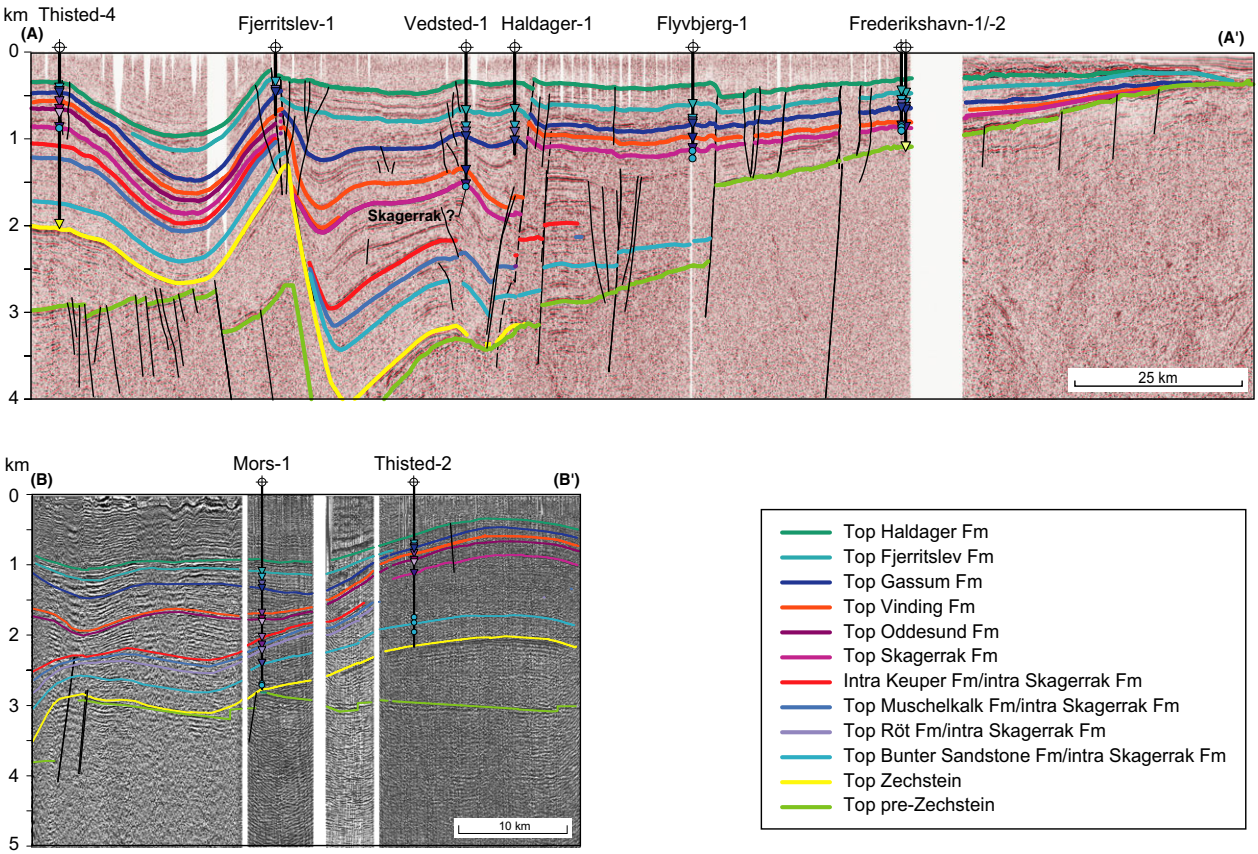

Fig. 2. (A) The seismic profile shows an east–west transition from the Danish Basin to the Skagerrak–Kattegat Platform (Fig. 1). The Skagerrak and Gassum formations and other Mesozoic sediments onlap the crystalline basement. (B) The seismic profile shows the influence of the underlying Zechstein salt due to movements into pillow-shaped accumulations or a transition to diapirism.

periods of deposition, subaerial exposure and fluvial re-deposition by migrating mega-ripples or linguoid bars in braided streams. Thin solitary mudstone and siltstone beds formed by suspension fall-out in temporarily abandoned channels, and desiccation cracks indicate occasional complete drying-out (Olsen, 1988). Occasional, fine- to medium-grained well-sorted sandstones with high-angle large-scale cross-bedding, wedge-shaped individual foresets and lagging intra-formational mudclasts are interpreted as aeolian deposits. Aeolian re-deposition of the braided stream deposits may have been a common process (Pedersen & Andersen, 1980).

The continental-dominated Triassic deposits have been subdivided into T-R sequences based on levels of maximum progradation and retrogradation, surfaces of basinward shift in facies and non-marine flooding (Fig. 3; Pedersen, 1998). Sequence 1 encompasses the lowermost part of the Skagerrak Formation in the north-eastern part of the basin consisting of sandstone-dominated fluvial deposits and the mudstone-dominated floodplain deposits. The sequence grades into lacustrine mudstones of the Bunter Shale Formation in the south-western part of the basin. Sequence 2 and 3 comprise the most sandstone-rich deposits of the fluvial part of the Skagerrak Formation in the north-eastern part of the basin, and the aeolian and ephemeral fluvial Bunter Sandstone Formation in the southern parts. Sequence 4 and 5 comprise the upper parts of the Skagerrak Formation in the north-eastern part of the basin and the evaporitic and argillaceous Röt Formation and successive carbonate deposits of the Muschelkalk Formation in the south-western part of the basin.

Depositional environment of the Gassum Formation

The Late Triassic to Early Jurassic Gassum Formation was deposited in a shallow marine embayment under the influence of a number of relative sea-level changes causing deposition of regressive shoreface sandstones and fluvial–estuarine sandstones encased in marine, lagoonal and lacustrine mudstones (Nielsen, 2003). The Gassum

Formation was originally interpreted as deltaic deposits (Larsen, 1966; Bertelsen, 1978). However, subsequent detailed sedimentological interpretation of well log patterns and a larger number of cores has enabled subdivision into six paralic and marine facies associations (Nielsen, 2003). Fluvial facies association overlies erosional surfaces and is dominated by light grey medium to coarse-grained large-scale cross-bedded sandstones (with claystone clasts and occasional pebbles at the base) in 2 to 14 m thick fining-upwards successions ending with carbonaceous claystones, or coaly beds with root traces, or cut by erosional surfaces. The lacustrine facies association mainly consists of massive to poorly laminated, micaceous silty dark grey claystones, with a poor non-marine palynomorphic assemblage (Bertelsen, 1978; Nielsen, Hamberg & Koppelhus in Nielsen, 1995). The estuarine channel facies association is characterized by light grey fine- to medium-grained sandstones with mudstone drapes on foresets in 5 to 25 m thick fining-upwards sequences, which are topped by coal beds or heterolithic units with rootlets. Significant incision occurred during sea-level lows, with some of these fluvial incised valleys subsequently filled with estuarine deposits (Hamberg, 1994). The lagoonal facies association consists of weakly bioturbated clay and sand-dominated heterolithic units, sandstones and carbonaceous claystones in sequences up to 11 m thick (Nielsen, 2003). The shoreface facies association comprise up to 30 m thick erosional-based successions of light grey, fine-grained hummocky cross-stratified lower shoreface sandstones and fine- to medium-grained sandstones with swaley cross-stratification, trough and planar cross-bedding, parallel and wave-ripple lamination, which are interpreted as upper shoreface, foreshore, swash-bars or beach deposits (Nielsen, 2003). The sandstones are capped by sharp transgressive surfaces of marine erosion overlain by muddy, burrowed, wave-rippled and wavy-bedded heterolithic units deposited in the offshore–shoreface transition zone. These repeated vertical facies successions reflect shoreline progradation during a stepwise forced regression in a shallow basin (Hamberg & Nielsen, 2000; Nielsen, 2003).

The formation is widely distributed with thicknesses of 50 to 150 m in the central and distal areas of the Danish part of the basin, although thickening associated with salt-structures and major faults occurs (up to 300 m in the Sorgenfrei–Tornquist Zone (Nielsen & Japsen, 1991). On the Skagerrak–Kattegat Platform the thickness decreases (10 to 80 m) and the formation is absent on most of the Ringkøbing–Fyn High due to later uplift and erosion (Nielsen, 2003).

The sediments were deposited during a series of relative sea-level fluctuations and are grouped into a number of depositional sequences, which shows that the deposition of sandstones gradually became limited to the north-eastern basin margin (Nielsen, 2003). Sequence Vi1 (Lower Norian–Lower Rhaetian) comprises the shallow marine mudstones of the Vinding Formation, lacustrine claystones and fluvial sandstones from the upper part of the Skagerrak Formation and marine mudstones, shoreface sandstones and estuarine deposits from the lower part of the Gassum Formation (Figs 1 and 2). The sequence is missing on the Skagerrak–Kattegat Platform. The subsequent sequence Ga1 (Lower Rhaetian–Lower Hettangian) consists of marine mudstones and shoreface, estuarine and fluvial sandstones from the upper part of the Gassum Formation, and centrally in the basin, also of the lowermost part of the marine mudstones of the Fjerritslev Formation. On the Skagerrak–Kattegat Platform, lacustrine mudstones from the uppermost part of the Skagerrak Formation are included in the sequence. Sequence Fj1 (Lower–Middle Hettangian) encompasses in the basin centre, the uppermost marine heterolithic part of the Gassum Formation and the marine mudstones of the lower part of the Fjerritslev Formation, which gradually becomes more sandstone-dominated towards north-east. The sequence consists only of the Gassum Formation in the Sorgenfrei–Tornquist Zone and on the Skagerrak–Kattegat Platform. The sequence Fj2 (Upper Hettangian–lowermost Sinemurian) consists of Gassum Formation sandstones along the north-eastern and eastern margin of the Sorgenfrei–Tornquist Zone. Marine mudstone and heteroliths of the Fjerritslev Formation dominate in the

Fig. 3. Heavy mineral abundance and U–Pb zircon ages for a number of sandstones are shown on the log panel of the Skagerrak and Gassum formations across the north-eastern part of the Norwegian–Danish Basin. The zircon ages document that they were primarily supplied from southern Norway and south-western Sweden in both the Skagerrak Formation and the Gassum Formation. The heavy mineral assemblage of the Skagerrak Formation is characterized by abundant hematite, titanomagnetite and unstable heavy minerals, even in the deeply buried parts, contrary to the more stable heavy mineral assemblage of abundant zircon, leucoxene and rutile in the Gassum Formation. The dominant zircon ages are generalized from Olivarius (2015) and Olivarius and Nielsen (2016) into a Norwegian group (Z : N), a Swedish group (Z : S) and a group of local reworked material (Z : R). 'Mafic minerals' comprise tourmaline, amphibole, pyroxene and olivine. The group 'Other' comprises titanite, sillimanite, kyanite, corundum, staurolite and various phosphate minerals. The log profile is flattened on the transgressive surface TS5, which follows the maximal progradation in the sequence Ga1. Lithostratigraphy is according to Pedersen (1998), Nielsen and Japsen (1991), Michelsen and Clausen (2002), and sequence stratigraphic correlation is according to Pedersen (1998) and Nielsen (2003). Data from adjacent wells are projected on the deepest log (i.e. samples from the Frederikshavn-2 well on the Frederikshavn-1 well log and comparable for Thisted-3/-4 and Stenlille-15/-19). Depths are measured present-day log depths (m b. K.B.) which are not corrected for uplift; core depths are corrected to log depths by shifting up to 10 m.

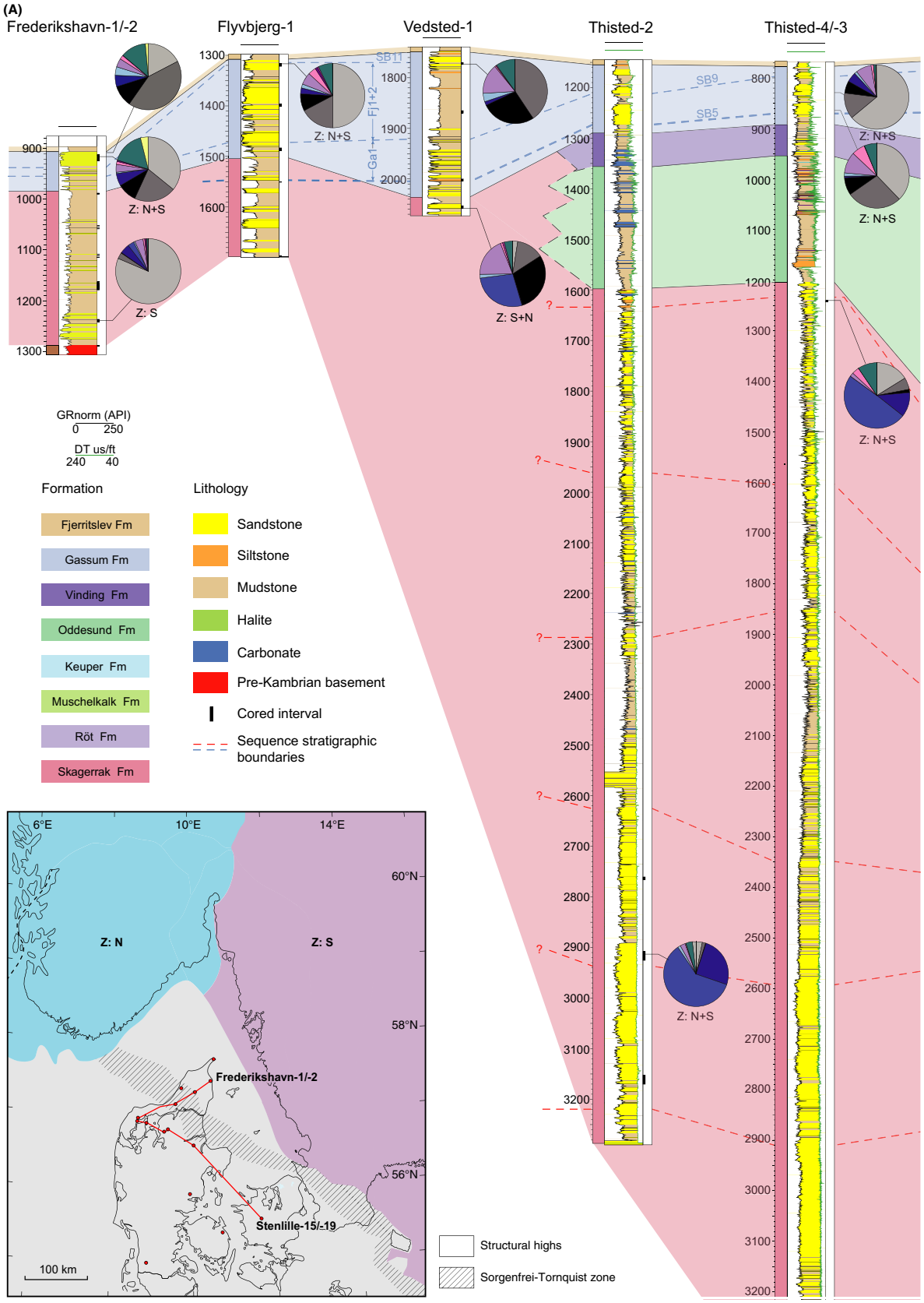

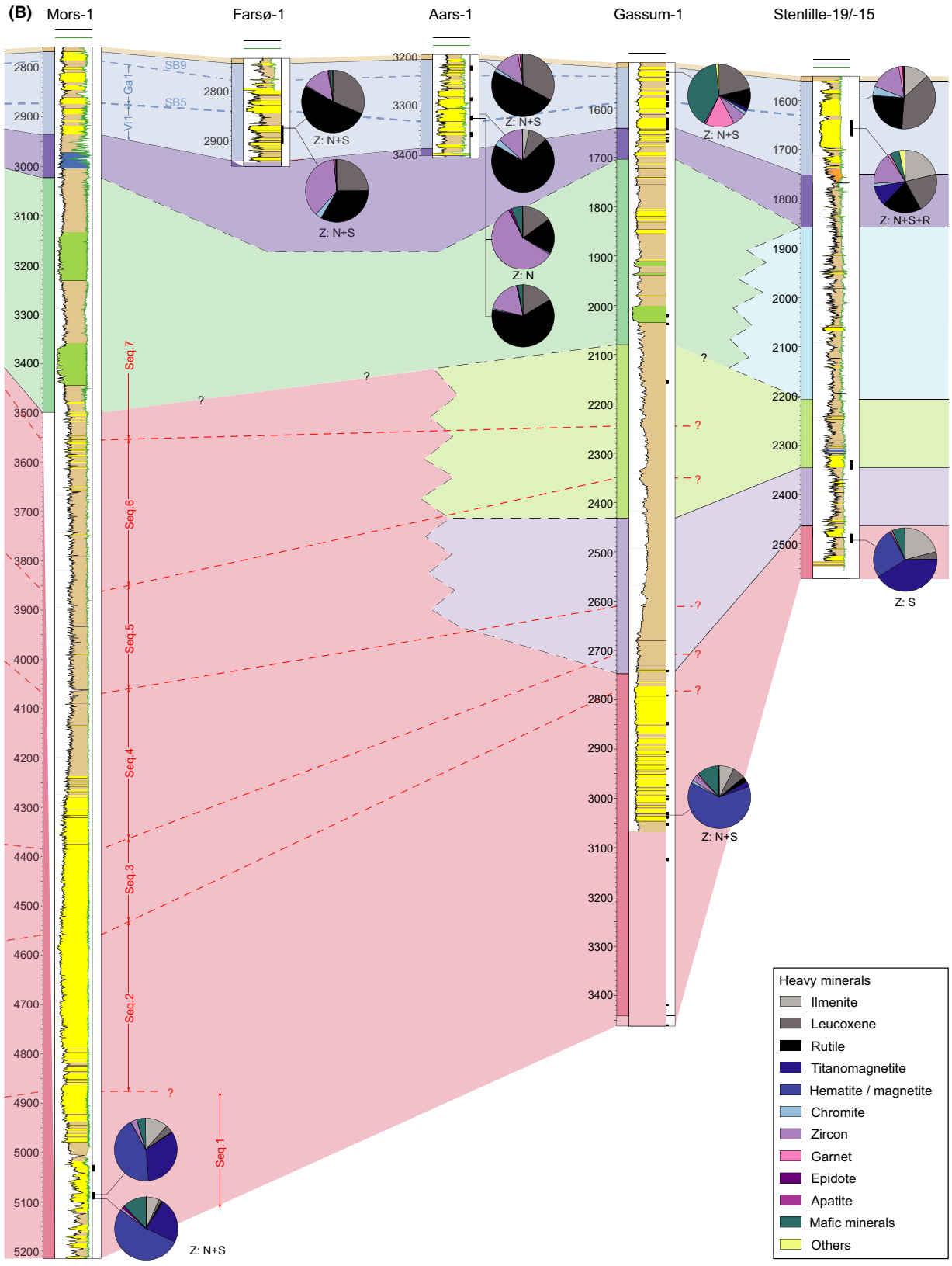

Fig. 3. Continued.

deeper parts of the basin. The sequence framework shows an overall marine transgression from TS1 to MFS1 followed by a general regression leading to the widespread and significant sequence boundary SB5 (Nielsen, 2003). Sediments beneath the sequence boundary SB5 were probably exposed to weathering and meteoric water flushing for a longer time than other parts of the Gassum Formation. After the exposure, an overall marine transgression followed (TS 5) culminating with the formation of the regional maximum flooding surface MFS7. Hereafter, a regression followed with the formation of SB9.

Climate

During Early and Middle Triassic, the Pangea continent was characterized by megamonsoonal climate, i.e. arid conditions temporarily interrupted by concentrated rainy periods (Kutzbach & Gallimore, 1989; Crowley & North, 1991; Parrish, 1993). The Norwegian–Danish Basin experienced an arid to semi-arid climate as it was situated approximately at 45°N during Late Triassic to Early Jurassic time according to palaeogeographic reconstructions (Ziegler, 1990). An arid to semi-arid climate during deposition of the Skagerrak Formation is consistent with the interfingering evaporitic deposits (Bertelsen, 1980). Drifting of the Pangea land mass towards more northern latitudes and breakup of the supercontinent opened the interior to seaways during the Rheatian which led to marine flooding and increased humidity in the surrounding areas (Manspeizer, 1994; Veevers, 1994; Ahlberg *et al.*, 2002; Francis, 2009). The climate thus shifted to humid during deposition of the Late Triassic to Early Jurassic, which is supported by the changed depositional style and the commonly embedded organic matter.

METHODS

Petrographical investigations are based on optical microscopy and scanning electron microscopy. The polished thin sections were impregnated with blue epoxy, for easy identification of porosity. Modal composition was obtained by point counting at least 500 grains, excluding pores, in thin sections. The thin sections were etched and stained with sodium cobaltinitrite in order to ensure fast identification of K-feldspar during point counting. Grain size and the degree of sorting were evaluated in each thin section. The Wentworth classification scheme provided the grain-size nomenclature (Wentworth, 1922), while sorting was estimated petrographically using the sorting comparators of Longiaru (1987), based on the sorting classes of Folk (1966). The sorting classes are defined for eight relative phi classes that range from very well to poorly sorted.

Supplementary studies of crystal morphologies and paragenetic relationships were performed on gold-coated rock chips mounted on stubs and on carbon-coated polished thin sections using a Phillips XL 40 scanning electron microscope using a secondary electron detector (SE) or back scatter electron detector (BSE). Energy-dispersive X-ray spectroscopy (EDS) analysis of detrital grains in thin sections verified the identification of feldspar during point counting. The electron beam was generated by a tungsten filament operating at 17 kV and 50 to 60 μA.

Computer-controlled scanning electron microscopy (CCSEM) of mounts of heavy mineral concentrates was run under similar operational conditions. The heavy minerals were liberated from the sandstone by machine crushing in a tungsten carbide mortar in several steps, each followed by removal of the fine fraction. The fraction 45 to 750 μm was removed by sieving. The heavy minerals were concentrated by heavy liquid separation using bromoform. The heavy mineral concentrates were embedded in epoxy and polished. Mineral identification was based on chemical composition obtained from EDS analysis using an in-house programme (Keulen *et al.*, 2012).

Petrographical investigations are supported by X-ray diffraction (XRD) of clay fraction and bulk rock samples. Powdered bulk rock samples were mounted with random orientation and scanned on an automated PANalytical X'Pert Pro MPD diffractometer with automatic divergence slit, using graphite monochromated CuKα radiation. Rietveld analysis of X-ray diffractograms was used for quantification of the major mineral phases in the bulk rock samples. The clay fraction was separated by sieving and gravitational settling, and prepared as smear slides. The smear slides were scanned on an automated Philips© PW 3710 X-ray diffractometer with automatic divergence slit, using graphite monochromated CuKα radiation. Clay specimens were scanned air-dried; ethylene glycolated at 60°C; and after heating at 500°C for 1 h. Criteria for identification of clay minerals can be found in Weibel (1999). Peak areas, corrected by diffractometer specific factors, were used to obtain a semi-quantitative estimate of the clay mineral abundance according to Hillier (2003).

Bulk rock carbon and oxygen isotope analyses were performed on carbon dioxide released from the carbonates after reaction with phosphoric acid at 25°C for 3 h and at 100°C overnight. This procedure ensures that the majority of the carbon dioxide produced at 25°C will be from calcite, while the carbon dioxide subsequently produced at 100°C will be mainly attributable to siderite. The fractionation factors used were from Rosenbaum & Sheppard (1986) and Friedman & O'Neil (1977). Oxygen and carbon

isotope data are presented in the standard δ notation relative to PDB, Pee Dee Belemnite (Craig, 1957).

Porosity and permeability were measured on well core plugs according to the API RP-40 standard (American Petroleum Institute, 1998). He-porosity was measured at unconfined conditions. Gas permeability was measured at a confining pressure of *ca* 2·8 MPa (400 psi), and at a mean N_2 gas pressure of *ca* 1·5 bar (bar absolute) = 0·15 MPa. Permeabilities below 0·05 mD were not measured or measured using a bubble flowmeter.

RESULTS

Analyses of the diagenetic changes in the Skagerrak and Gassum formations are based on petrographical investigations (Figs 4 to 11) and are supported by heavy mineral analyses (Figs 3, 6 and 7), clay mineralogy (Fig. 11) and carbonate isotopic analyses (Fig. 12). The differences between the diagenesis of sandstones deposited in arid and humid climates, respectively, are compared in the figures (Figs 6 to 11) and compiled in Table 1.

Petrographical investigations

Skagerrak Formation (arid–semi-arid conditions)

Detrital composition

The alluvial fan deposits of the Skagerrak Formation consist of moderately to poorly sorted conglomerates, fine-grained sandstones or siltstone, whereas the braided stream deposits consist of well-sorted fine- to medium-grained sandstones. The sandstones are dominated by arkoses, lithic arkoses and subarkoses (Fig. 4) according to the classification scheme of McBride (1963). Monocrystalline quartz, with subordinate polycrystalline quartz, comprises the major part of the framework grains. With regard to the braided stream sandstones, the feldspar group is dominated by K-feldspar, and plagioclase is only rarely identified. In contrast, Ca-rich plagioclase and albite occur in the alluvial fan deposits. Alteration of feldspar grains includes dissolution, clay mineral replacement or carbonate replacement and sericitization. The rock fragments are mainly igneous and rarely metamorphic, but volcanic rock fragments are common in lowermost Triassic – Sequence 1 and 3 in the Mors-1 and Thisted-2 cores. Intra-formational clay intraclasts are abundant in few samples. Mica occurs in small amounts in most samples and may show signs of oxidation, replacement by clay minerals, or minor expansion due to precipitation of authigenic phases (hematite and anatase) between their cleavage planes.

Hematite (including hematized magnetite) and titanomagnetite dominate the heavy mineral assemblage in the deeply buried and most distal deposited parts of the Skagerrak Formation (Figs 3 and 6; Weibel, 1998). Ilmenite is generally most common in the shallowly buried and proximal parts of the Skagerrak Formation (Figs 3), and in the deeper buried sandstones it may show dissolution features (Fig. 6). Garnet disappears with increased burial depth (Fig. 7). Zircon and rutile vary in abundance, but are typically concurrent (Figs 3 and 7). Generally ilmenite and leucoxene dominate the heavy mineral assemblage, except for one sample from the Vedsted-1 well, which has a relatively mature heavy mineral assemblage, dominated by zircon and rutile.

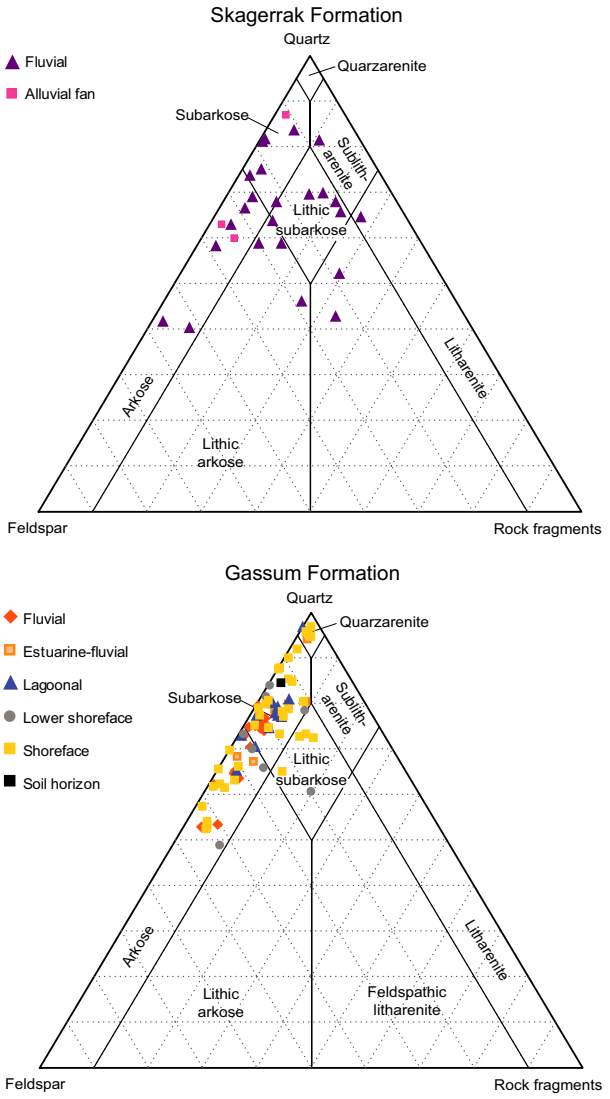

Fig. 4. The Skagerrak Formation shows varying sandstone compositions of subarkoses, lithic arkoses, lithic subarkoses and feldspatic litharenites, whereas the Gassum Formation is dominated by subarkoses and arkoses. Sandstone types are based on modal analysis and plotted according to the classification by McBride (1963).

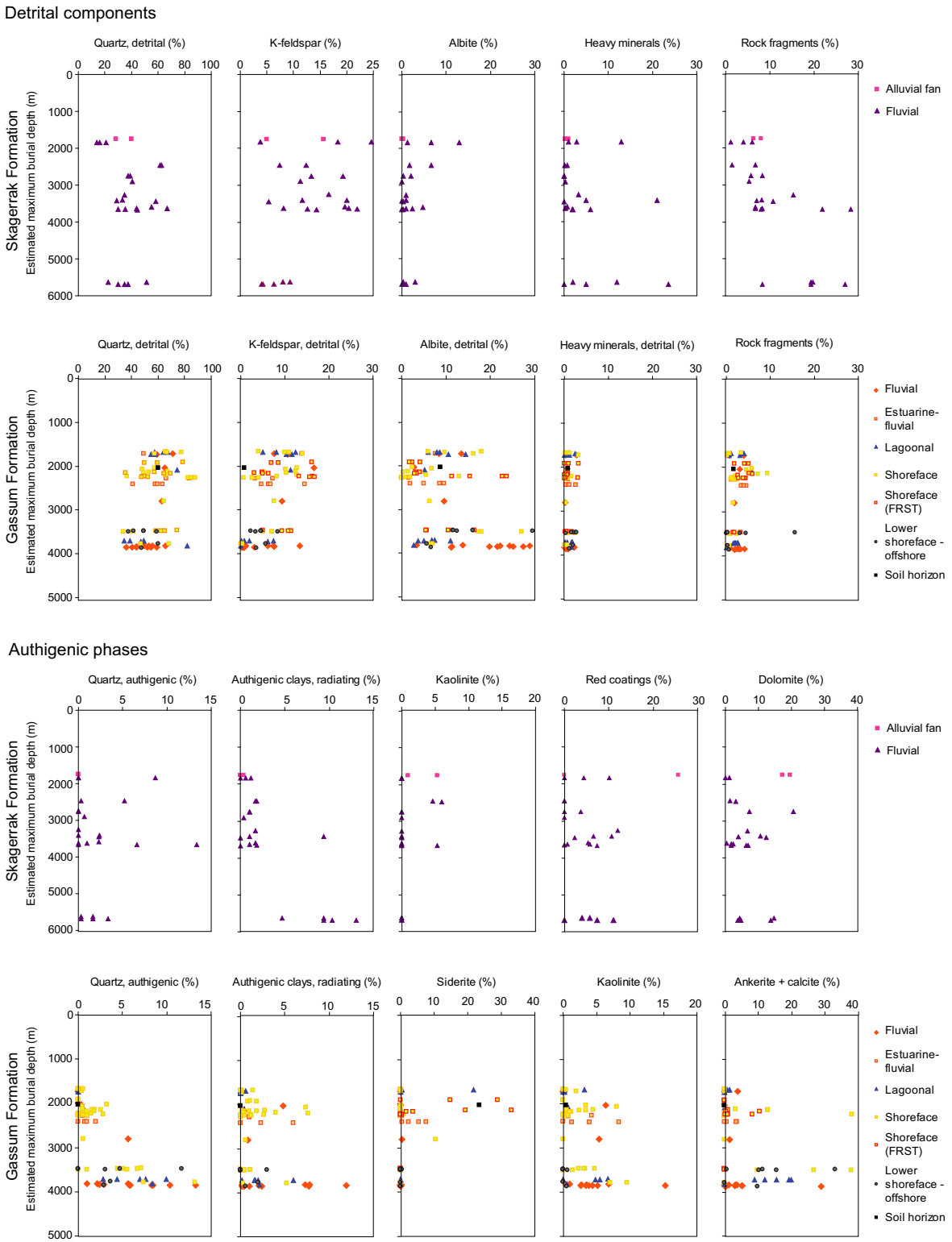

Fig. 5. Modal abundance of the dominant minerals in the Skagerrak and Gassum formations plotted versus estimated maximum burial depth. The Skagerrak Formation shows no clear mineralogical variation with increased burial depth. In contrast, the Gassum Formation shows increasing abundance of detrital albite, authigenic quartz and ankerite cement and decreasing abundance of authigenic siderite with increasing burial depth. The maximum burial depth is present day burial depth corrected for Neogene uplift (Japsen and Bidstrup 1999; Japsen et al. 2007).

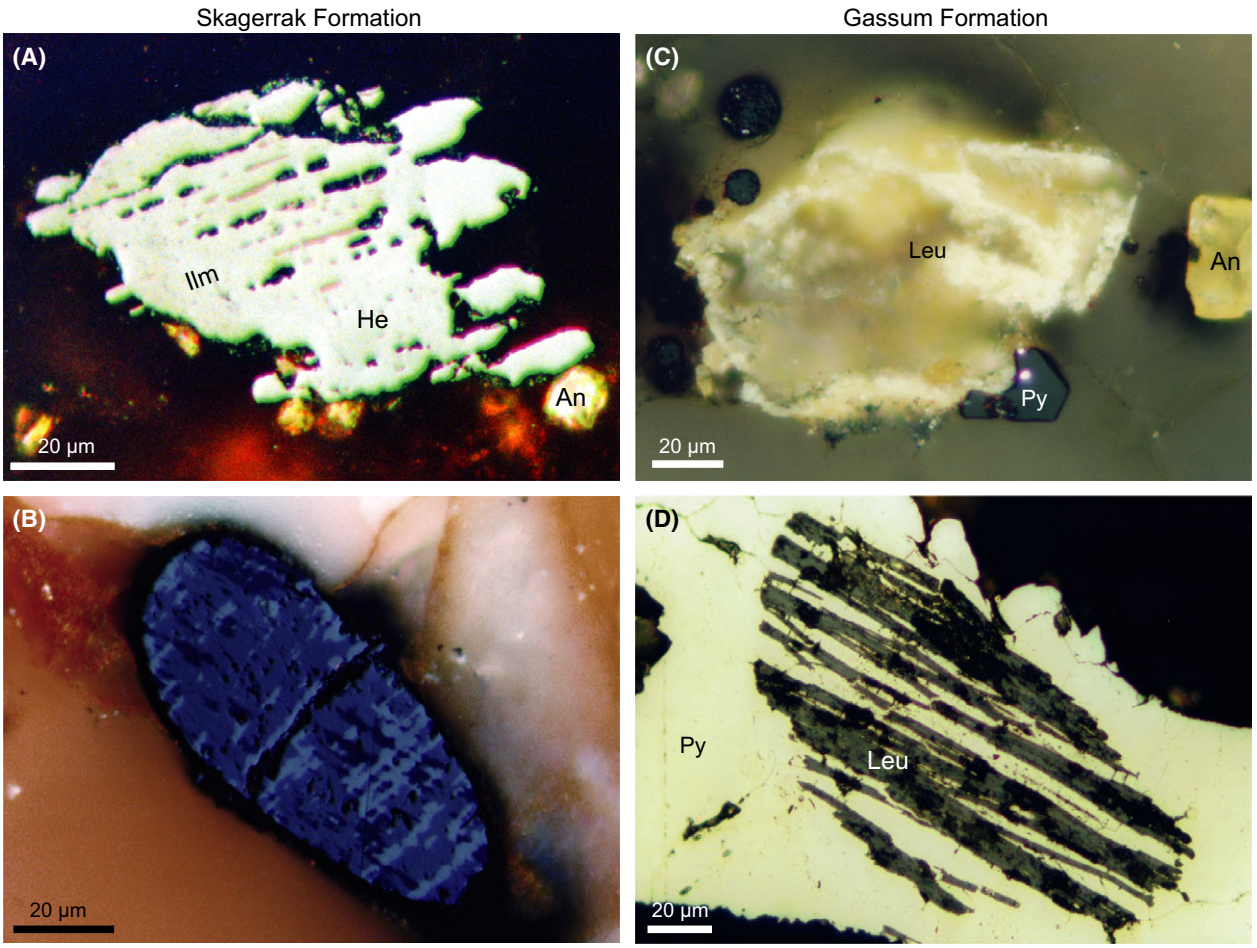

Fig. 6. (A) Preferential dissolution of ilmenite (Ilm) exsolution lamellae in unaffected hematite host (He) promotes precipitation of anatase (An) in the pore space, Skagerrak Formation, Gassum-1 well, 2850·29 m, reflected light, oil immersion. (B) Hematized magnetite with crystals orientated in three different directions reflecting the crystallography of magnetite, Skagerrak Formation, Gassum-1 well, 2995·89 m, reflected light, oil immersion, crossed nicols. (C) Leucoxene (Leu) replacement of ilmenite associated with pyrite (Py) and anatase (An) precipitation in the pore space, Gassum Formation, Gassum-1 well, 1634·44 m, reflected light, oil immersion, crossed nicols. (D) Ilmenite grain, which is replaced by leucoxene (Leu) and pyrite (Py) and enclosed in concretionary pyrite, Gassum Formation, reflected light, oil immersion, Gassum Formation, Gassum-1 well, 1640·45 m, reflected light, oil immersion.

Authigenic phases

Coatings of iron-oxide/hydroxide cover most detrital grains and in places occur between authigenic phases, such as clays, dolomite and quartz (Figs 8B, 9B, and 10C). Additionally, authigenic hematite occurs in various forms: replacement of magnetite (Fig. 6B), amphibole and mica, syntaxial overgrowths on detrital hematite, tiny crystals between cleavage planes in mica or arranged in pore-filling rosettes. Authigenic titanium oxides comprise leucoxene, which replaces detrital Fe-Ti oxides, and single crystals of anatase, which precipitated in the pore space close to altered Ti-rich grains.

Clay minerals occur tangentially (infiltration clays) in the shallowly buried alluvial fan deposits, contrary to the radiating pore-lining clays and clay replacement of unstable grains in the intermediately and deeply buried braided stream sandstones (Fig. 8A). The honey-comb textured clay coatings of mixed-layer illite/smectite and fibrous illite is particularly abundant in the deepest buried sandstones (Fig. 8C). Pore-lining illitic clays are succeeded by pore-filling Mg-rich chloritic clays, which occasionally are clearly separated from the previous illitic pore-lining clays by red coatings (Fig. 8B).

Carbonate cement consists mainly of dolomite and occasionally of calcite in sandstones of shallow or intermediate burial depth. Calcite as calcrete cement occurs only in the shallowly buried alluvial fan deposits (Fig. 9A). Calcite cement preferentially occurs as micritic cement. Calcite commonly exhibits several of the calcrete

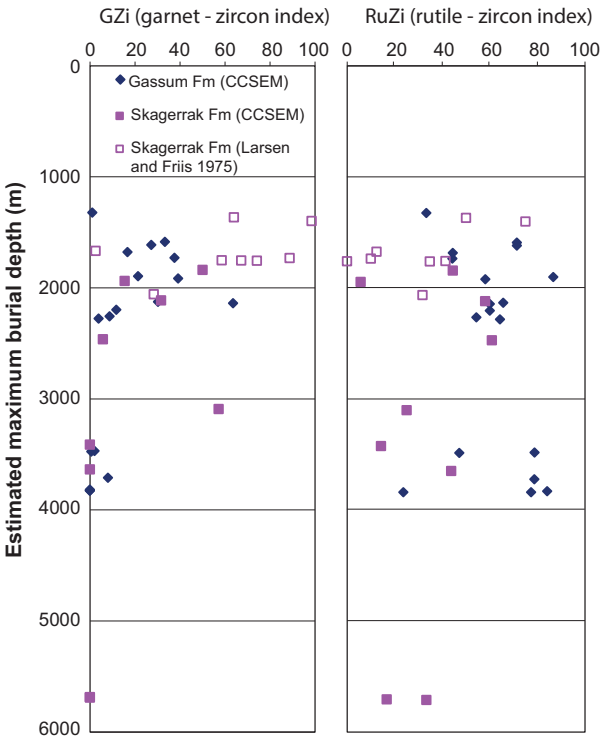

Fig. 7. The Skagerrak Formation has a less mature heavy mineral assemblage than the Gassum Formation, which is shown by a generally higher rutile-zircon index (RuZi) than for the Skagerrak Formation. Disappearance of garnet with burial depth, i.e. low garnet-zircon index (GZi) is independent of climate. Heavy mineral indexes are calculated according to Morton and Hallsworth (1999).

fabric elements (Wright, 1990), as calcite corrodes the rims of the detrital minerals, that "float" in the calcite matrix, and forms radiating rims around detrital grains in samples of shallow depth (e.g. Frederikshavn-1, -2, Skagen-2 and Flyvbjerg-1). Dolomite occurs as pore-filling poikilotopic and micritic cement and as rhombohedral-shaped crystals with distinct growth zones (Fig. 9B). Poikilotopic dolomite cement may have a radiating extinction thereby resembling saddle dolomite. The micritic cement preferentially forms between cleavage planes of expanded mica, whereas rhombohedral crystals commonly grow inside intra-formational clay clasts. Ankerite cement is only recognized in one well (Vedsted-1), where it occurs as pore-filling poikilotopic cement.

Anhydrite is very rare in the Skagerrak Formation. It is the last precipitating phase and may be corrosive to other mineral phases. Anhydrite fills relatively large pores – oversize pores, which suggest replacement of another mineral or an earlier cement (Fig. 9C).

Authigenic K-feldspar occurs as common syntaxial and rare epitaxial overgrowths on detrital feldspar grains and as crystals precipitated on remnants of dissolved feldspars in the secondary porosity (Fig. 10A). Authigenic feldspar encloses red coatings and illitic rims. K-feldspar overgrowths are more abundant than quartz overgrowths in some of the sandstones (Gassum-1 well, 2153·51 m; Thisted-2 well, 2764·62 m).

Authigenic quartz occurs as syntaxial prismatic outgrowths or pore-filling overgrowths (macroquartz). Prismatic quartz outgrowths preferentially occur where relatively thick clay rims or red coatings cover the detrital grains (Fig. 10B; e.g. the Mors-1 and Thisted-2 wells). Pore-filling quartz overgrowths dominate rare, fine-grained sandstones and sandstones with thin pore-lining clay coatings (e.g. the Gassum-1 well). Authigenic quartz encloses other authigenic phases, such as red coatings, anatase, illite rims and fibrous illite, feldspar and early rhombohedral carbonate.

Gassum Formation (well-vegetated, humid conditions)

Detrital composition

The Gassum Formation is characterized by well-sorted fine- to medium-grained sandstone with scattered organic matter. Rare bi-modal sorting of the sand occurs in samples from the Vedsted-1 well. The sandstones are mainly subarkoses and arkoses (Fig. 4) according to the classification by McBride (1963). Monocrystalline quartz, with subordinate polycrystalline quartz, dominates the framework grains. Feldspar abundance varies across the studied part of the Norwegian–Danish Basin with feldspar relatively more abundant in the north-western part than in the eastern part. K-feldspar is the dominant feldspar in the shallowly buried parts of the Gassum Formation, whereas albite and K-feldspar occur in equal amounts in the intermediately buried parts of the Gassum Formation (i.e. the Gassum-1, Fjerritslev-2 and Vedsted-1 wells), and albite dominates the feldspar group in the deepest buried parts (i.e. Aars-1 and Farsø-1 wells) (Fig. 5). The feldspar grains have experienced variable alterations, from partial dissolution, replacement by kaolinite or carbonate to albitization in the deepest buried parts. Some oversize pores containing kaolinite or clay-lining moulds ("ghost rims") are inferred to be remnants after completely dissolved feldspar grains. Rock fragments comprising plutonic, micaceous metamorphic and sedimentary rock fragments are generally rare. The highest abundance of rock fragments occurs in the lower shoreface deposits. Plutonic rock fragments are generally more abundant than other types of rock fragments in the majority of the Gassum Formation. Mica, dominated by muscovite and with subordinate biotite and chlorite, occurs in all samples. Mica shows varying degree of

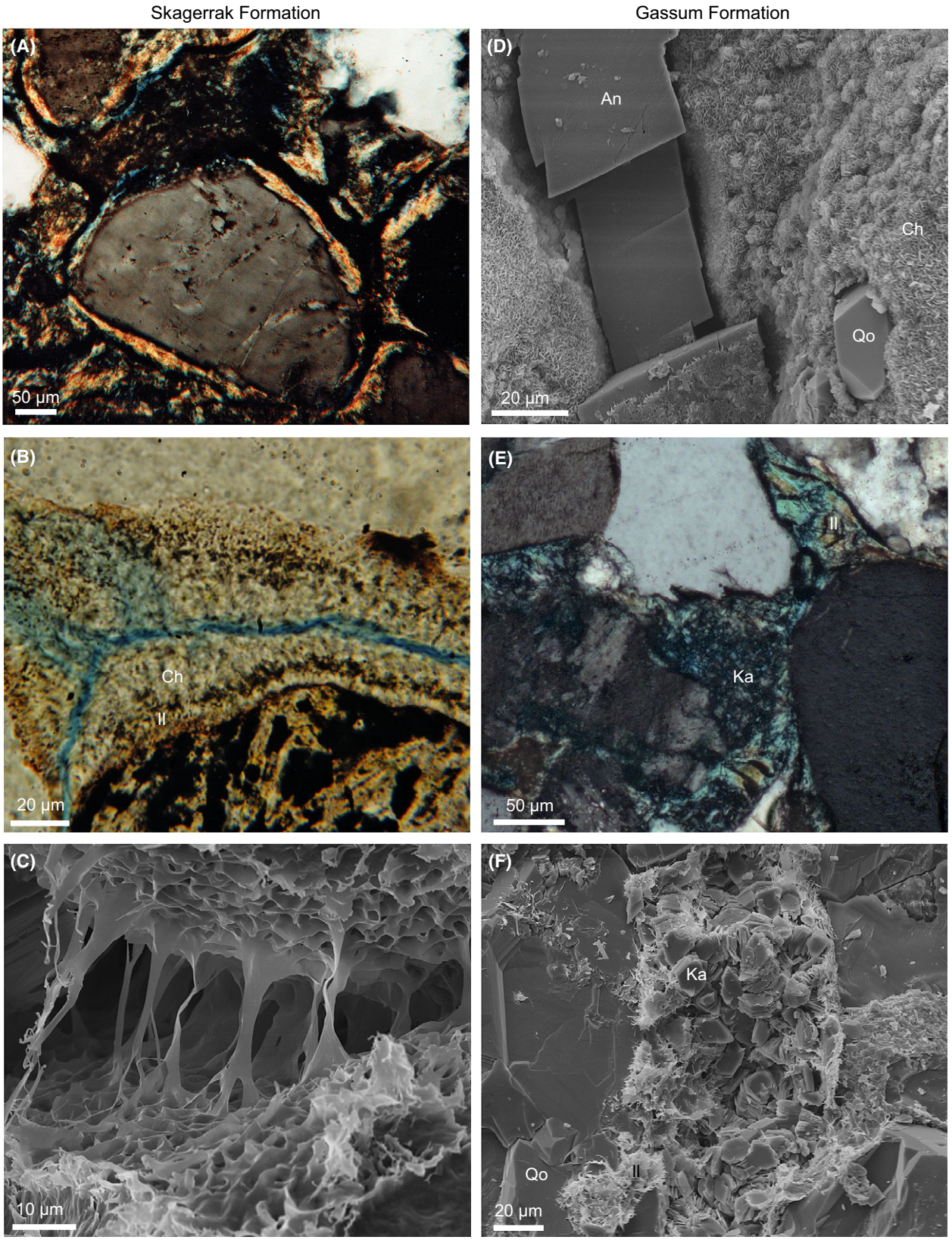

Fig. 8. (A) Infiltration clays surrounding detrital grains, Skagerrak Formation, alluvial fan deposits, Sæby-1 well, 1628·03 m, crossed nicols. (B) Primarily red coatings enclosed in pore-lining illite (Il) succeeded by a secondary red coating and pore-filling chlorite (Ch) show that oxidizing conditions continued after precipitation of illite, Skagerrak Formation, Mors-1 well, 5090·32 m, crossed nicols. (C) Honey-comb textured clay coating show that smectite formed in the arid to semi-arid climate before its transformation into mixed layer illite/smectite during burial finalizing with protruding growth of pore bridging illite fibres, Skagerrak Formation, Thisted-2 well, 2761·60 m, Scanning electron micrograph. (D) Thin continuous Fe-rich chlorite coatings (Ch) prior to quartz overgrowth (Qo) and ankerite cement (An) show completely different clay minerals formed in estuarine–fluvial environment in a humid climate, Gassum Formation, Vedsted-1 well, 1775·58 m, Scanning electron micrograph. (E) Pore-filling kaolinite (Ka) and pore-filling and pore-lining illitic clays (Il) with high birefringence, which may originate from illitization of kaolinitic detrital clays, Aars-1 well, 3326·49 m, crossed nicols. (F) Pore-lining illitic clays (Il) partly enclosed in authigenic quartz (Qo) and pore-filling kaolinite (Ka), Gassum Formation, Aars-1 well, 3353·05 m, Scanning electron micrograph.

alteration, exhibiting either expansion along cleavage planes caused by precipitation of authigenic minerals (e.g. siderite or kaolinite) or compaction along stylolites in the deepest wells.

The heavy mineral assemblage is of completely different composition in the shallowly buried sandstones from the Skagerrak and Gassum formations (Fig. 3). Ilmenite dominates the heavy minerals assemblage in the shallowly buried parts of the Gassum Formation, whereas rutile and leucoxene generally dominate the deeper buried parts (Figs 3 and 7). Leucoxene replacement of ilmenite is common in the Gassum Formation (Fig. 6). During burial, the least stable heavy minerals are altered; therefore, the relative proportion of the stable heavy minerals such as rutile, leucoxene and zircon increases in the deeply buried parts of the Gassum Formation (Fig. 7). The general trend seems to be that the abundance of the relatively unstable heavy minerals, garnet and mafic minerals decreases in the most distal and deeply buried parts of the Gassum Formation. However, this varies somewhat locally and one sample from the Gassum-1 well has a high content of mafic minerals and garnet (Fig. 3), in addition to abundant micaceous metamorphic rock fragments. Deeply buried lagoonal deposits have the lowest abundance of unstable heavy minerals (e.g. mafic minerals, epidote and garnet), whereas deeply buried shoreface sediments often have a low content of mafic minerals.

Authigenic phases

Siderite is the first authigenic phase and can be highly abundant in shallowly buried sandstones, although it is generally rare in deeply buried parts of the Gassum Formation (Fig. 5), where it is mainly found enclosed in ankerite cement. Siderite occurs as numerous small rhombohedral crystals (up to 15 μm) and occasionally as displacive spherulites (Fig. 9D and E). Rhombohedral siderite initiates between cleavage planes of mica (preferentially biotite or chlorite) and results in expansion of the micas. Siderite is Mg rich in most samples (offshore, shoreface and fluvial deposits) except for one sample from a soil horizon (in the Børglum-1 well) where siderite is Mn rich.

Pyrite framboids precipitate during early diagenesis more or less simultaneously with the siderite rhombs, as pyrite framboids grow on siderite rhombs or are enclosed in them (e.g. Fig. 9D and E). Pyrite occurs as three phases, first framboids, secondary euhedral crystals followed by tertiary pore-filling cement. Euhedral pyrite crystals enclose pyrite framboids, siderite and kaolinite booklets. Pore-filling pyrite cement commonly encloses partly dissolved K-feldspar grains. Pyrite is commonly associated with organic matter or altered Fe-bearing minerals, as for example ilmenite replaced by leucoxene.

Kaolinite occurs in two crystal sizes, booklets of relatively large (5 to 10 μm) single crystals and fine crystals (1 to 2 μm). Kaolinite booklets fill secondary (oversize) pores and primary pores adjacent to altered feldspar grains. Fine kaolinite crystals grow between the cleavage planes of mica, in particular muscovite, and form in adjacent pores. Kaolinite booklets may be enclosed in euhedral pyrite crystals, authigenic quartz and ankerite. Compression and deformation of kaolinite in oversize pores show that compaction continued after kaolinite precipitation.

Continuous coatings of fine chlorite crystals (1 to 2 μm) on all detrital grains (including recycled kaolinite) are characteristic of sandstones from the forced regressive system tract of Sequence Fj2 (Figs 3 and 8D), which is cored in the Vedsted-1 and Flyvbjerg-1 wells. Irregularly distributed chlorite intergrown with later illite is typical in intensively bioturbated samples. Sandstones in other forced regressive systems tracts of Sequence Fj1 or Vi1 (Farsø-1 and Børglum-1 wells) have chlorite coatings intergrown with illite, and do not have the characteristic continuous thin chlorite coatings. A low degree of bioturbation coincides with the continuous chlorite coating on sand grains.

Fibrous illite grows between authigenic chlorite and from coatings of detrital clays. Illite is commonly seen spread out in the open pores of the deepest buried sandstones (e.g. Aars-1 well), suggesting illite replacement of kaolinitized mica or tangential detrital clays (Fig. 8E).

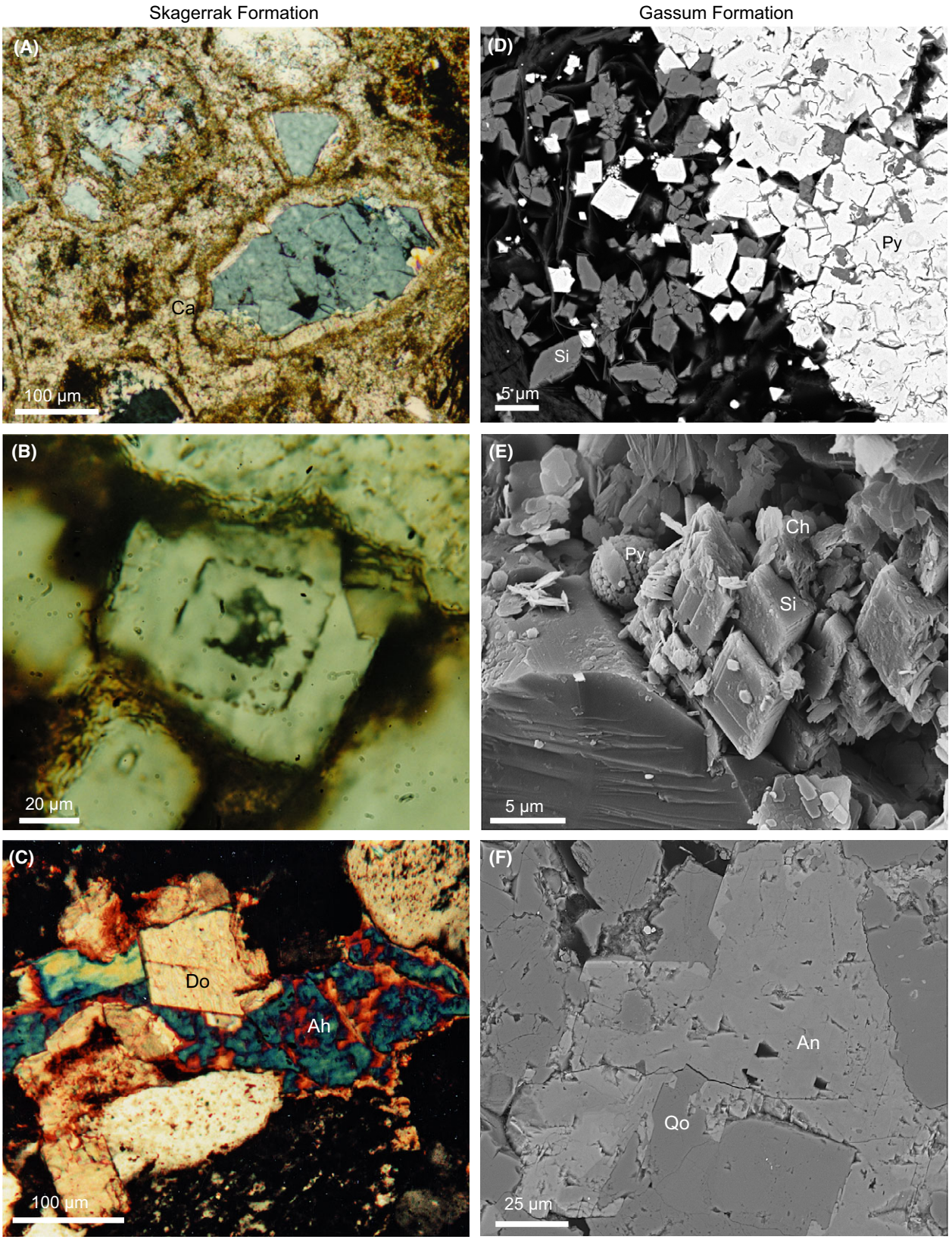

Fig. 9. (A) Calcrete calcite (Ca) cement indicating a pedogenetic origin in an arid to semi-arid climate, Skagerrak Formation, Frederikshavn-2 well, 1050·95 m, crossed nicols. (B) Dolomite rhomb consisting of two episodes of precipitation separated by a red coating, which shows that oxidizing conditions continued after the initial precipitation of dolomite, Skagerrak Formation, Gassum-1 well, 2155·95 m. (C) Anhydrite cement (Ah) in oversize pore indicates replacement of an early diagenetic cement, possibly evaporative precipitated gypsum, whereas enclosure of dolomite cement (Do) suggest a later recrystallization, Skagerrak Formation, Thisted-2 well, 2763·04 m, crossed nicols. (D) Siderite rhombs (Si) enclosed in cubic pyrite (Py) show that here the sulphide-reducing conditions followed the iron reducing, Gassum Formation, Frederikshavn-2 well, 885·85 m, Backscatter electron micrograph. (E) Pyrite framboid (Py) and siderite rhombs (Si) partly covered by chlorite crystals (Ch) show the co-occurrence of several Fe-rich phases formed in a relatively short time interval, Gassum Formation, Vedsted-1 well, 2009·69 m, Scanning electron micrograph. (F) Pore-filling ankerite (An) enclosing quartz overgrowths (Qo), which shows that ankerite is a late diagenetic phase. Gassum Formation, Farsø-1 well, 2894·66 m, Backscatter electron micrograph.

Albitization of K-feldspar and possibly also of plagioclase increases in abundance with burial depth (Fig. 5). Albitization of K-feldspar is followed by albite overgrowths, and authigenic albite precipitates on remnants after partly dissolved K-feldspar grains (Fig. 10D).

Carbonate is mainly sparry in fluvial and lagoonal deposits (e.g. the Aars-1 well), poikilotopic in shoreface and offshore deposits (the Farsø-1 well) and occasionally micritic in lagoonal deposits. Additionally, rhombohedrons (typically of calcite or siderite) appear in sporadic cemented sandstones. The carbonate type is burial depth, so calcite cement commonly dominates in the shallowly buried sandstones, whereas ankerite and ferroan dolomite occur in the deeply buried sandstones (Fig. 5). The carbonate types may vary according to the depositional environment, as exemplified by the Gassum-1 core, which is dominated by calcite in the upper shoreface deposits of the lowermost part of the Gassum Formation, whereas siderite and ankerite cement in the uppermost part where multiple shifts occur in depositional environments, from foreshore, shoreface and transitions to offshore characterize the uppermost part of the core, whereas a consistent upper shoreface deposit dominates in the lower part. The pore-filling sparry ankerite and ferroan dolomite can be corrosive towards all other minerals or may partly replace them. Ankerite cement encloses albite remnants after partly dissolved feldspar grains, possibly Ca-rich plagioclase. Ankerite cement is the last authigenic phase, which encloses quartz overgrowths and barite crystals (Fig. 9F).

Syntaxial quartz overgrowths are the dominant occurrence of authigenic quartz, which increases in abundance with increasing burial depth (Fig. 5). Completely intergrown quartz overgrowths occur in deeply buried sandstones (e.g. the Aars-1 and Farsø-1 wells, Fig. 10E). Quartz overgrowths may be partly inhibited by chloritic/illitic coatings and occasionally, prismatic quartz outgrowths occur in sandstones having thick Fe-rich chloritic coatings. Sutured grain-to-grain contact and stylolites developed along mica concentrations appear in some deeply buried sandstones (e.g. the Farsø-1 and Aars-1 cores; Fig. 10F). Barite needles or pore-filling cement is a late diagenetic phase, which encloses quartz overgrowths, but is enclosed in ankerite.

Clay minerals

The shallowly buried sandstones of the Gassum Formation generally have a clay mineral assemblage of kaolinite ≫ illite > chlorite > mixed-layer illite/smectite, whereas the deeply buried sandstones have more abundant illite = kaolinite, illite ≫ chlorite. The mudstones and the heterolithic bedded sandstones of the Gassum Formation generally have a clay mineral assemblage of illite > kaolinite ≫ chlorite. The sandstones of the Gassum Formation have higher kaolinite contents than the heterolithic bedded sandstones and intercalated mudstones, which results in a much higher kaolinite/illite ratio for the sandstones (Fig. 11). The Skagerrak Formation is characterized by a very low kaolinite/illite ratio compared with the Gassum Formation (Fig. 11). The sandstones of the Skagerrak Formation typically have a clay mineral assemblage of smectite ≫ mixed-layer smectite/illite ≫ palygorskite and illite in the shallowly buried parts, whereas the order of abundance changes in the deeply buried parts to illite ≫ chlorite > mixed-layer illite/smectite in the deeply buried parts (Weibel, 1999). Reduction spots or reduced parts of the Skagerrak generally have a high content of kaolinite and it is noteworthy that these samples plot together with the Gassum Formation.

Oxygen and carbon isotopic composition

Skagerrak Formation

Dolomite cement has oxygen isotopic values ranging from −11·2 to −2·8‰ $\delta^{18}O_{PDB}$ and calcite cement has oxygen isotopic values of −10·4 to −7·6‰ $\delta^{18}O_{PDB}$ (Fig. 12).

Precipitation temperatures are estimated according to the carbonate fractionation factors of Zeng (1999) and a formation water isotopic composition of −1·25 $\delta^{18}O_{PDB}$ as measured in Skagerrak Formation water sampled in the Thisted-2 well. As the isotopic composition of the formation water is obtained at maximum burial depth,

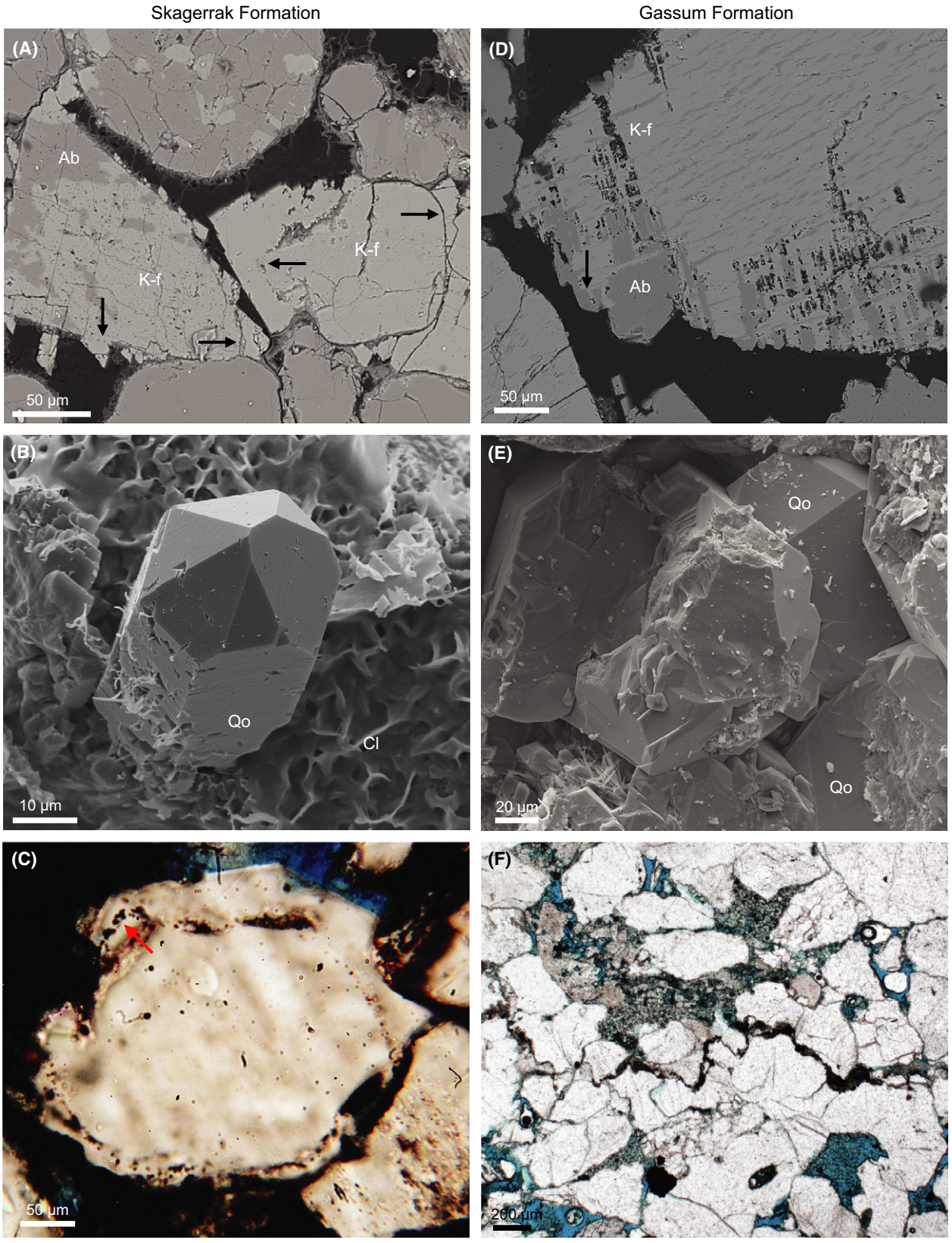

Fig. 10. (A) K-feldspar overgrowth, locally limited by clay coatings, but with no dissolution features, shows that K-feldspar is stable in the Skagerrak Formation during deep burial, Thisted-2 well, 2761·60 m, Backscatter electron micrograph. (B) Quartz outgrowth precipitation caused by limited access to the detrital quartz grain due to continuous iron-oxides/hydroxide and clay coating (Cl) on the detrital grain, Skagerrak Formation, Thisted-2 well, 2763·40 m, Scanning electron micrograph. (C) Two episodes of quartz precipitation separated by iron-oxides/hydroxides (the second is marked by a white arrow) shows that oxidizing conditions remained during burial, Skagerrak Formation, Gassum-1 well, 2524·75 m. (D) Small albite overgrowth and intragranular albitization shows that albite is the stable feldspar in the Gassum Formation during burial, Farsø-1, 2869·85 m, Backscatter electron micrograph. (E) Quartz overgrowths are extensive in the Gassum Formation as clay coatings are typically irregular and not continuous, Aars-1 well, 3208·45 m, Scanning electron micrograph. (F) Stylolites formed prior to dissolution of detrital feldspar grains, Aars-1 well, 3277·45 m.

temperature estimates are only tentative. Dolomite cement may have precipitation temperatures of 40 to 80°C using the fractionation factor of Zeng (1999), and calcite cement may have precipitated as temperatures of 60 to 80°C according to the fractionation factor of Horibe & Oba (1972) or Zeng (1999).

Gassum Formation

Siderite rhombs have an oxygen isotopic composition varying from −8·7 to −1·8‰ $\delta^{18}O_{PDB}$ (Fig. 12). Calcite cement has oxygen isotope values of −12·9 to −7·6‰ $\delta^{18}O_{PDB}$ that almost corresponds to the values of calcite cement in the Skagerrak Formation. Ankerite and Fe-dolomite cement have oxygen isotopic values of −11·9 to −9·7‰ $\delta^{18}O_{PDB}$ and −12·0 to −6·1‰ $\delta^{18}O_{PDB}$ (Fig. 12).

The siderite precipitation temperature is estimated to 30 to 40°C according to the fractionation factor of Carothers *et al.* (1988) and a formation water isotopic composition of −0·5 $\delta^{18}O_{SMOW}$ as measured in formation water in the marine deposits of the Gassum Formation in the Farsø-1 well. The exception is soil horizons, for which −5 $\delta^{18}O_{PDB}$ is applied, which is characteristic of sphaerosiderite in Lower Jurassic fluvial deposits from Scania (Weibel *et al.*, 2016) (Fig. 12). The calcite precipitation temperatures are estimated to 60 to 100°C using the fractionation factor of Horibe & Oba (1972) or Zeng (1999), whereas ankerite and Fe-dolomite are estimated to have formed at 110 to 130°C, using the fractionation factors of Zeng (1999) and the formation water isotopic composition of −0·5 $\delta^{18}O_{SMOW}$.

Porosity and permeability variations

Skagerrak Formation

The coarse-grained fluvial sandstones have a higher permeability relative to porosity than medium- and fine-grained sandstones (Fig. 13A). The medium-grained sandstones form a dual trends with one group having almost similar permeabilities (1·4 to 566 mD for the Skagerrak Formation, in general, at porosities <20%) as the coarse-grained sandstones, and the other group showing remarkably lower permeabilities (0·2 to 32 mD for the Skagerrak Formation in the Thisted-2 core at porosities <20%) compared to the coarse-grained sandstones. The alluvial sandstones have a porosity–permeability trend lying between the fine-grained and medium fluvial sandstones (Fig. 13B). The group of medium-grained sandstones with low permeability is characterized by a relatively high content of illitic clays (>5%) (Fig. 13A). Kaolinite may seemingly be present in amounts >5% without causing a major reduction in permeability. In cases where the presence of illite cannot explain low permeabilities, the low porosity and permeability are commonly associated with a combination of quartz overgrowths and dolomite/calcite cement.

Gassum Formation

In general, coarse-grained sandstones have a higher permeability at a specific porosity than the medium-, fine- and very fine-grained sandstones, which can be observed as notably different trend for each grain size in Fig. 13E at porosities >20%. The permeability can be relatively high even in quartz-cemented sandstones (57 to 1138 mD), whereas ankerite/calcite cement seems to reduce both permeability (0·03 to 21 mD) and porosity (3 to 11%) (Fig. 13C, D, and E). Siderite cement reduces permeability relative to porosity even more than other carbonate types and siderite-cemented shoreface sandstones therefore form the lowermost permeability–porosity trend in Fig. 13E. Illitic clays result in relatively low permeability, in particular for fluvial sandstones in the Gassum Formation. In most cases, kaolinite reduces the permeability less than other clay types (Fig. 13B).

Comparison of the two formations is slightly complicated by the variation in number of samples representing the different depositional environments; therefore, the porosity and permeability of the fluvial sandstones deposited under arid to semi-arid conditions are compared with both fluvial, estuarine-fluvial and shoreface sandstones deposited under humid conditions. Sandstone samples of shallow burial depth typically have high porosities (>20%). The corresponding permeabilities are almost equally good for sandstones deposited under arid to semi-arid (Skagerrak Formation) and humid

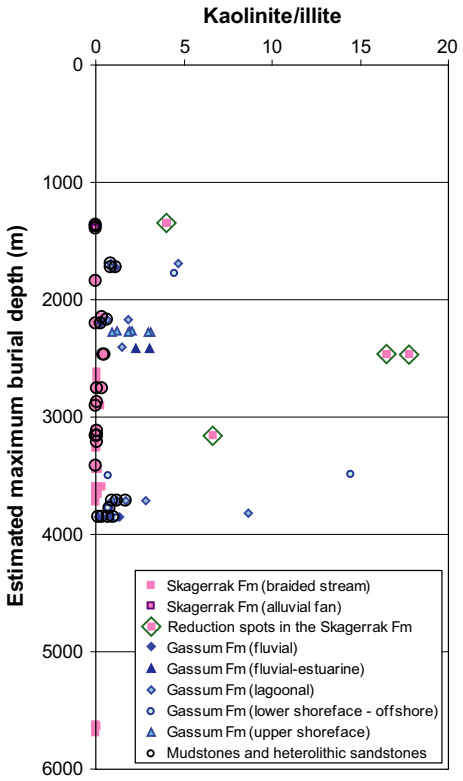

Fig. 11. The kaolinite/illite ratio, based on X-ray diffraction of the clay fraction, is clearly different between the Skagerrak and Gassum formations with the exception of Skagerrak Formation samples from the reduction spots, which plot together with the Gassum Formation. Encircled samples from the Skagerrak Formation represent reduction spots.

conditions (Gassum Formation), although the latter may have higher maximum values. The permeabilities in the Gassum Formation are 340 to 8080 mD and 100 to 8640 mD in coarse- and medium-grained shoreface sandstones, respectively, and 290 to 670 mD in medium-grained fluvial sandstones (Fig. 13C, D, and E). Almost equally high permeabilities occur in the Skagerrak Formation, with 820 to 3750 mD and 600 to 2820 mD in coarse- and medium-grained fluvial sandstones, respectively. Deeply buried sandstones, which roughly have porosities <20%, show higher maximum permeabilities (4 to 820 mD and 0·2 to 560 mD for coarse- and medium-

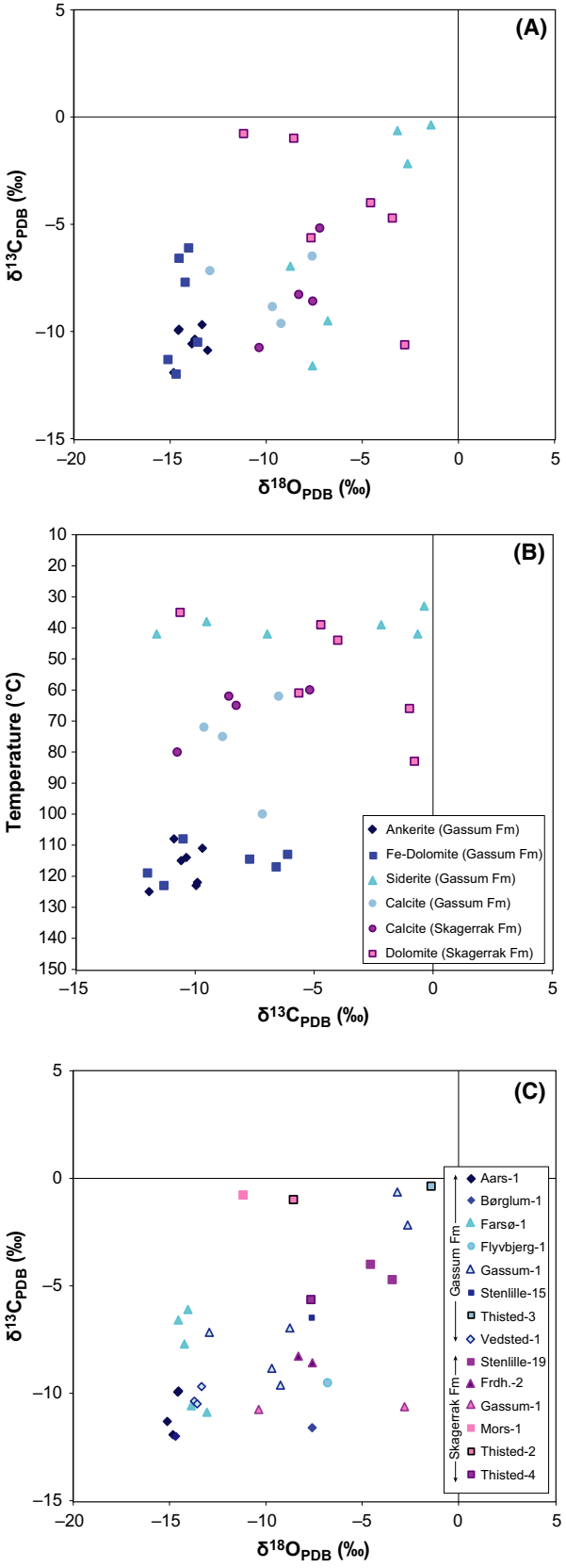

Fig. 12. Stable isotopic composition of carbonate cement from the Skagerrak and Gassum formations. (A) $\delta^{13}C_{PDB}$ is plotted against $\delta^{18}O_{PDB}$ for the data set subdivided according to carbonate type in each formation. (B) Estimated temperatures are plotted against $\delta^{13}C_{PDB}$ for the data set subdivided according to carbonate type in each formation. (C) $\delta^{13}C_{PDB}$ is plotted versus $\delta^{18}O_{PDB}$ for the data set subdivided according to well location. The legend is identical for A and B.

Table 1. Comparable mineralogical and diagenetic characteristics of the Skagerrak and Gassum Formation, which are compiled from previous studies (Larsen, 1966; Larsen and Friis, 1975; Friis, 1987; Weibel, 1998, 1999; Weibel & Groberty, 1999; Weibel & Friis, 2004, 2007; Weibel *et al.*, 2017)

	Arid to semi-arid climatic conditions (Skagerrak Formation)	Humid climatic conditions (Gassum Formation)
Detrital		
Quartz	Dominant, unaltered	Dominant Unaltered in shallowly buried samples Unaltered or occasionally dissolved along stylolites in deeply buried samples
K-feldspar	Unaltered?	Dissolved and replaced by kaolinite at shallow burial, alibitization at deeper burial K-feldspar remnants in pore-filling pyrite cement
Albite	Dissolved?	Dissolved and replaced by kaolinite at shallow burial Precipitation at deeper burial
Mica	Unaltered red or hematized	Replaced by kaolinite or pyritized
Glauconite	Oxidized red margins	Unaltered
Ilmenite	Replaced by leucoxene and has promoted anatase crystals in the open pores	Replaced by leucoxene and has promoted anatase crystals in the open pores
Magnetite	Replaced by hematite	Dissolved or altered to pyrite or siderite
Hematite	Unaltered	Dissolved or altered to pyrite or siderite
Titanomagnetite	Replaced by leucoxene and has promoted anatase crystals in the open pores	Replaced by leucoxene and has promoted anatase crystals in the open pores
Apatite	Rare	Absent (never deposited or dissolved?)
Epidote	Common with dissolution features	Rare
Tourmaline	Common, unaltered	Common, unaltered
Authigenic		
Carbonate cement	Calcite at shallow burial depth Dolomite in deeply buried samples	Siderite in shallowly buried samples Calcite in shallowly–intermediately buried samples Ankerite in deeply buried samples
Feldspar	K-feldspar	Albite and albitization
Quartz	Prismatic outgrowths Syntaxial overgrowths	Syntaxial overgrowths Stylolites
Smectite	Common in shallowly buried parts	Rare
Illite and illitic clays	Common as transformation of smectite	Common as replacement of kaolinite
Chlorite	Late Mg-rich chlorite	Early Fe-rich chlorite
Kaolinite	Rare except for reduction spots	Kaolinite is the dominant clay mineral
Fe-rich phases	Goethite in shallowly buried samples Hematite in deeply buried samples	Pyrite (or siderite) Marcasite?
Sulphate	Anhydrite	Barite

grained sandstones, respectively) in fluvial sandstones of the Skagerrak Formation than coarse-grained shoreface and fluvial sandstone of the Gassum Formation, characterized by permeabilities of 0·3 to 220 mD and 0·4 to 15 mD, respectively.

DISCUSSION

Sediment source area

The Precambrian Fennoscandian Shield was the major sediment source area of both the Skagerrak and Gassum formations (Larsen, 1966; Larsen & Friis, 1975; Olivarius, 2015; Olivarius & Nielsen, 2016). Basement rocks of identical ages were eroded and deposited in the basin, as zircon grains of ages reflecting the same Fennoscandian terrains appear in both formations (Fig. 3). Local variations in the supplied material have been recognized, for example the south-easternmost part of the basin was influenced by a local sediment supply of very stable heavy minerals, which originate from recycling of sediments exposed on the Ringkøbing–Fyn High during deposition of the Gassum Formation (Larsen, 1966; Olivarius, 2015). In a similar way, the northernmost part of the Norwegian–Danish Basin is influenced by a local sediment source of abundant titanite, which was active during deposition of both the Skagerrak and Gassum formations (Larsen, 1966; Larsen & Friis, 1975). The CCSEM heavy mineral analysis carried out in this study cannot confirm the presence of relatively large proportions of titanite in

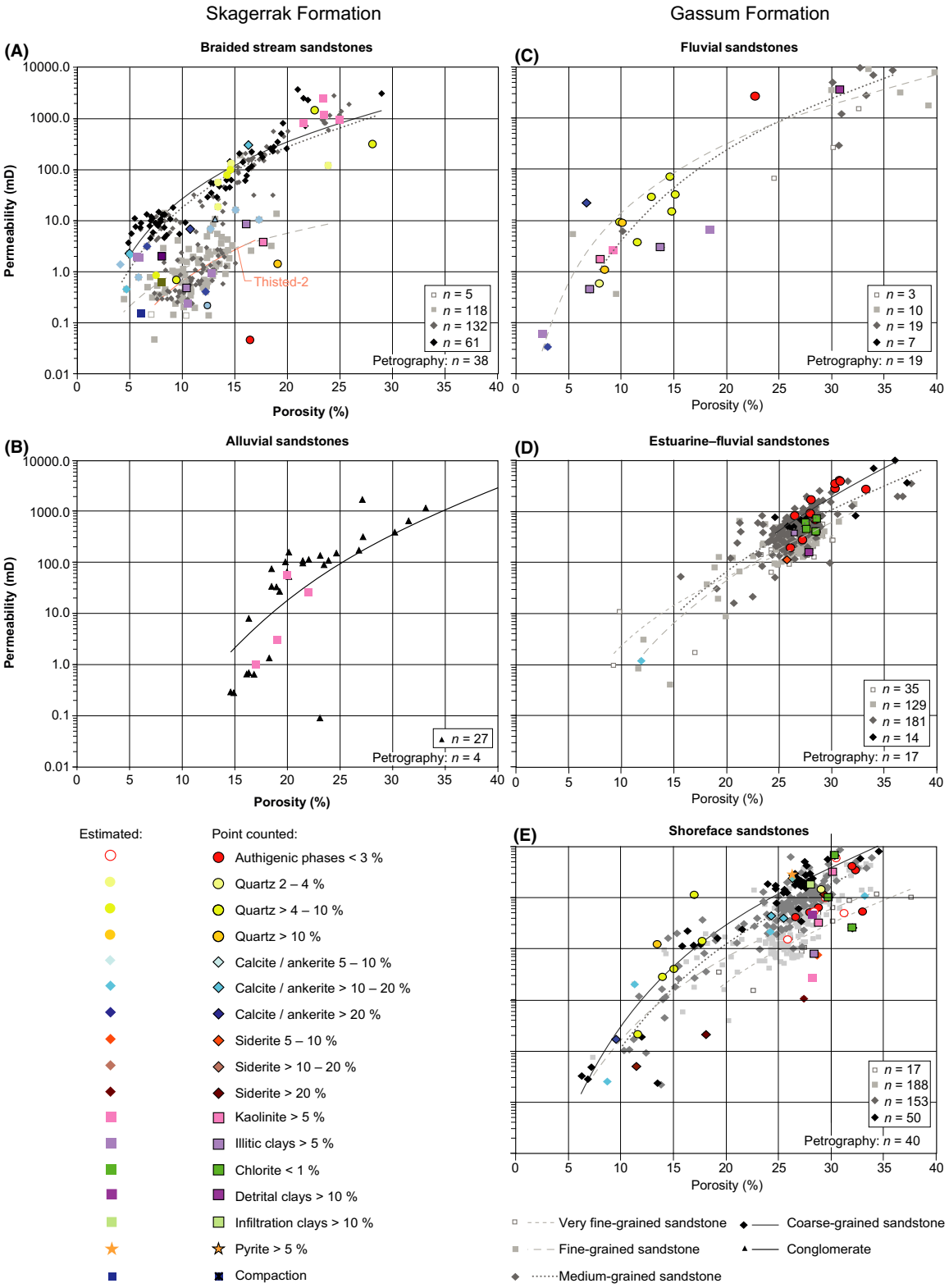

Fig. 13. Porosity versus permeability for plug samples from the Skagerrak Formation divided into braided stream sandstones (A) and alluvial fan deposits (B), compared with samples from the Gassum Formation (Weibel et al. 2017) of fluvial (C), estuarine–fluvial (D) and shoreface (E) depositional environments. Note, that medium-grained sandstones from the Thisted-2 core in (A) forms another trend (marked by orange) than the remaining medium-grained sandstones of the Skagerrak Formation. Petrographically investigated samples are shown by their dominant diagenetic changes. 'Chlorite' is here specified as thin continuous chlorite coatings, whereas illitic clays comprise a mixture of illite and chlorite.

the northernmost part of the basin (Fig. 3). This may be due to two factors, (i) low counting of rare transparent heavy minerals by the CCSEM method as opaque minerals dominate and (ii) erroneous identification of titanite due to optical resemblance between monazite and Fe-containing titanite (Deer *et al.*, 1985).

Apatite occurs in rare amounts in the Skagerrak Formation, but is absent in the Gassum Formation. The rare occurrence of apatite may reflect its low abundance in the sediment source area (Fennoscandian), as younger sediments sourced from the same area are also characterized by a remarkably low apatite content (Friis, 1976, 1978). Even fossiliferous apatite is apparently absent in the Gassum Formation despite its partly marine origin. This reflects intensive weathering of the sediment during transport and immediately after deposition, as apatite is particularly unstable with regard to weathering, whereas it is stable during burial diagenesis (Friis, 1976, 1978; Morton, 1986; Morton & Hallsworth, 1999).

Different climates resulted in variable weathering products and sediment composition in the area of deposition. Despite having the same sediment source area, the heavy mineral suite varies between the Skagerrak and Gassum formations, both in the shallowly and deeply buried parts (Fig. 3). The Gassum Formation is typically characterized by more than 50% ilmenite and leucoxene, whereas the Skagerrak Formation may have either a high ilmenite or hematite (and rare magnetite) content (Fig. 3). Epidote and garnet with delicate dissolution features and fragile leucoxene grains or leucoxene in trellis texture show that much of the alteration occurred after deposition (Larsen, 1966; Larsen & Friis, 1975; Weibel, 1998; Weibel & Friis, 2004, 2007). Additionally, more rock fragments, including the least stable volcanic rock fragments, survived the weathering in the source area and subsequent transportation during the arid to semi-arid climate of the Skagerrak Formation than did during the humid climate of the Gassum Formation (Fig. 4).

Climate-induced early diagenesis

Arid to semi-arid climate

Immature material was supplied from the sediment source area during the arid to semi-arid climate, and is today partly preserved in the shallowly buried parts of the Skagerrak Formation. Alteration of ilmenite into leucoxene commenced at a slow rate, so ilmenite, although partly altered to leucoxene, is preserved in the Skagerrak Formation even in the deepest buried parts (estimated burial depth of 5700 m; Fig. 3). In addition, the Skagerrak Formation is characterized by infiltration clays of smectite, randomly ordered mixed-layer smectite–illite and illite, which is in agreement with the immature composition of the sediment supplied to the basin (Weibel, 1999). Ca-rich plagioclases occur solely in the alluvial fan deposits in the northernmost part of the basin (i.e. the Sæby-1 well), and their intensive degree of alteration to kaolinite suggests that they may previously have been equally abundant in the alluvial fans as albite and K-feldspar. Kaolinite is a common alteration product of both feldspar and mica in these alluvial fan deposits, suggesting that the alluvial fans may have developed during relatively more humid episodes (Christenson & Purcell, 1985; Dorn *et al.*, 1987; Dorn, 2013). Thus, an increased precipitation in the areas of alluvial fan deposition compared to other areas could explain both the formation of kaolinite and the generally reduced conditions in the alluvial fans, caused by more abundant organic matter.

In the remaining part of the basin, oxidizing conditions prevailed in the arid to semi-arid climate and evaporative processes were active during early diagenesis. Early diagenetic oxidizing conditions are documented by the almost ubiquitous red grain coatings formed by iron-oxide/hydroxides, goethite in the shallowly buried sandstones (Weibel, 1998, 1999; Weibel & Groberty, 1999). Hematite relics are absent in reduction spots in the Skagerrak Formation, where locally reducing conditions were created immediately after deposition, similar to observation from the reduction spots in other red beds (Bensing *et al.*, 2005). Consequently, the reddening process seems to be associated with oxidizing conditions in this case. However, red coloration in other sandstones may origin from *in situ* soil formation (Mora *et al.*, 1998), eroded lateritic soils (Van Houten, 1961), ferruginization associated with fluctuating groundwater level, and hence iron mobilization under reducing conditions and precipitation under oxidizing conditions (Besly *et al.*, 1993; Mücke, 1994) or from iron-oxides formed due to microbial activity in siderite-cemented sandstones (Burgess *et al.*, 2016). Reddish oxidation rims in recycled glauconite grains and iron-oxide/hydroxide replacement of Fe-rich mica and

heavy minerals confirm the overall oxidizing conditions. Intense evaporation and pedogenetic processes promoted formation of calcrete and the rare late diagenetic anhydrite present in oversize pores may have had an early diagenetic gypsum precursor, which formed due to evaporation of pore fluids (Fig. 9A and C). Calcrete either never formed in the braided stream deposits, only in the alluvial fan deposits, or recrystallization and growth of larger crystals at the expense of smaller may have taken place at deeper burial depths. The latter explanation is supported by the isotopic composition of calcite cement (Fig. 12), which resembles that of caliche and pedogenetic carbonate in desert environments (Cerling & Quade, 1993; Quade *et al.*, 2007). The samples from the Stenlille-19 and Thisted-4 wells have an oxygen isotopic composition that resembles pedogenetic carbonate of recent deserts having low annual precipitation, whereas the calcite cement in the Frederikshavn-2 well could have formed in a desert environment having slightly higher annual precipitation (Cerling & Quade, 1993; Quade *et al.*, 2007). This fits well with the inferred position of these wells during deposition of the Skagerrak Formation, as the alluvial fan deposits in the Frederikshavn-2 well were located closest to the highland, whereas the Thisted-4 and Stenlille-19 wells were situated more basinwards with probably lower precipitation and a higher degree of evaporation (Figs 1 and 2).

Humid well-vegetated climate

Relatively mature material was supplied from the Fennoscandian Shield during the humid climate governing deposition of the Gassum Formation. The high intensity of weathering is also shown by the highly stable minerals, zircon, rutile and tourmaline dominating the heavy mineral suite and by the alteration of ilmenite into leucoxene (Fig. 3; Larsen & Friis, 1975; Weibel & Friis, 2007).

The presence of organic matter controls several early diagenetic processes, as it serves as an energy source for microbes and creates reducing conditions, under which iron is highly soluble. Siderite and pyrite occur in Gassum Formation sandstones, with chlorite coatings, pyrite as a rare phase (*ca* 2%) and siderite less abundant (2 to 5%) than would otherwise be the case (up to 30%). Thus, although iron competitive, these three Fe-rich phases are not mutually exclusive.

Sulphate-reducing bacteria promoted the precipitation of pyrite framboids, as seen by their preferential occurrence near organic matter. Sulphate concentration in the pore fluids was probably the limiting factor for pyrite precipitation, as iron-oxides and hydroxides are unstable under reducing conditions and likely to be dissolved and transported to places of sulphate reduction (Berner, 1969; Canfield *et al.*, 1992). Textural evidence suggests that altered Fe-Ti oxides acted as an internal iron source for euhedral pyrite in the Gassum Formation, but only where other iron sources were limited. Concretionary pyrite (in the Aars-1 well) formed beneath a marine (transgressive) erosional boundary and this interval has remained in the sulphate-reducing regime for a longer period than comparative sediments. Other Fe-rich phases precipitated, when the sulphate source was exhausted, and the sediments entered the methanogenic regime.

The very early diagenetic precipitation of siderite is documented by its displacive growth between mica cleavage planes and its interaction with pyrite framboids (Fig. 8). Siderite oxygen isotopic composition ($\delta^{18}O_{PDB}$: $-8{\cdot}7$ to $-1{\cdot}8‰$) corresponds with burial temperatures of 33 to 42°C according to the siderite-water fractionation factor by Carothers *et al.* (1988) and a formation water composition of $-0{\cdot}5‰$ $\delta^{18}O_{PDB}$ for marine sandstones and $-5‰$ $\delta^{18}O_{PDB}$ for soil horizons (Fig. 12). Alternating pyrite and siderite precipitation can be associated with small changes in pH and Eh and/or variations in CO_3^{2-} or H_2S saturation (Coleman & Raiswell, 1981). Sulphate-reducing bacteria can, under specific conditions (in a consortium with microbial fermenters), reduce Fe^{3+} using hydrogen, formed during fermentation, instead of sulphate (Coleman, 1993). During bacterial sulphate reduction, simple organic molecules (CH_2O) are oxidized to inorganic aqueous carbonate, e.g. HCO_3^-, which can precipitate as carbonate minerals, which may include siderite if the Fe-supply is sufficient. In this way, the same sulphate-reducing bacteria may promote formation of pyrite or siderite depending on the associated microbial activity. Mica may have liberated iron during its alteration, or served as a protective site for the bacteria colony, which could explain the numerous siderite crystals that precipitate between the mica cleavage planes and result in expansion of mica to several times its original size. When organic matter was deposited together with mica, then both an energy source for the bacteria and an internal Fe electron receptor was present, which resulted in intensively siderite-cemented sandstones.

The continuous chlorite coatings formed only in estuarine-fluvial and upper shoreface sandstones from the forced regressive system tract (Nielsen, 2003; Weibel *et al.*, 2017). At this time, rivers from the north-east entered an estuary where clay coatings may have formed on detrital grains (Griffiths *et al.*, 2015). After re-deposition in the outer estuary or shoreface environment during forced regression, the clay coatings may have recrystallized to form berthierine, odinite or smectite coatings. Eventually, during burial, these clay minerals were transformed into Fe-rich chlorite (Odin, 1985; Hillier, 1994;

Kazerouni *et al.*, 2013). This recycling of the sediments during a relative sea-level fall could have promoted the precipitation of glauconite (and glauconitization of mica) and may explain the co-occurrence of chloritized kaolinite and fresh authigenic kaolinite.

Kaolinite formed at the expense of feldspar and muscovite at shallow burial depth (Figs 5, 9E and F). The high precipitation in the humid climate rendered the possibility of flushing of diluted meteoric water through the sandstones and removal of soluble species, whereas less soluble species such as Si and Al were precipitated as kaolinite (Bjørlykke, 1984, 1998; Bjørlykke & Aagaard, 1992). Kaolinite precipitation, promoted by meteoric water, probably occurred in fluvial, estuarine-fluvial, lagoonal and even shoreface sandstones, if forced into the latter by a hydraulic head (Bjørlykke & Aagaard, 1992). Meteoric water flushing may have intensified during shoreline progradation associated with relative sea-level falls (Burley, 1984; Ketzer *et al.*, 2003; Ruffel *et al.*, 2003; El-ghali *et al.*, 2009), which occurred several time during deposition of the Gassum Formation (Nielsen, 2003).

Climate affected burial diagenesis

Although weathering in the sediment source area has a major influence on the heavy mineral assemblage, diagenesis is equally important. Garnet disappears in deeply buried parts of the Skagerrak and Gassum formations (Fig. 7), as it becomes unstable at elevated temperatures (Morton, 1984; Morton & Hallsworth, 1999). Epidote and mafic minerals are present in shallowly buried (<2500 m estimated maximum burial depth) parts of the Gassum Formation, but are rare in deeply buried parts (>2500 m) (Fig. 3). Fluvial sandstones from the deepest buried parts provide the only exception to this overall trend by having a limited mafic mineral content. Fluvial deposits may have abundant and more varied suites of heavy minerals compared to other settings (Dill, 1998). Ilmenite, epidote and mafic minerals are present both in the shallowly and deeply buried parts of the Skagerrak Formation, showing that the typical heavy mineral alteration is reduced in the Skagerrak Formation due to the higher content of unstable minerals, and probably also to more saline initial pore fluids compared with the Gassum Formation.

Sediments deposited under semi-arid to arid conditions – Skagerrak Formation

The composition of red coatings change from goethite in shallowly buried sandstones to hematite during deeper burial and was accompanied by haematization of iron-rich minerals (magnetite, biotite and heavy minerals) and direct precipitation of hematite overgrowths (Fig. 6B). Pseudomorphic transformation of goethite into hematite initiated at 57°C and was completed at 105°C in the Skagerrak Formation (Weibel, 1999; Weibel & Groberty, 1999). This shows that the oxidizing conditions that prevailed immediately after deposition remained during early burial, at least until the first precipitation of both quartz overgrowths, dolomite overgrowths and after pore-lining illite (Figs 8B, 9B and 10C). The first quartz precipitation was prismatic outgrowths, which reflects limited access to detrital quartz grain surfaces due to the thick red coatings and clay rims (Burley, 1984; Fisher *et al.*, 2000). Precipitation of quartz outgrowths may begin at 60°C (Weibel *et al.*, 2010) but quartz precipitation has its maximum at 90 to 100°C (Walderhaug, 1990; Giles *et al.*, 1992; Gluyas *et al.*, 1993; Storvoll *et al.*, 2002; Mansurbeg *et al.*, 2008; Bjørlykke *et al.*, 2009), and it is within this temperature interval that the larger quartz overgrowths formed, as the deeper buried sandstones experienced temperatures of 105 to 150°C at maximum burial depth (Weibel, 1999). At increased burial, silica was supplied from rock fragments and feldspar alteration, clay mineral diagenesis and sutured grain-to-grain contacts in the sandstones having the lowest content of ductile fragments (mica and rock fragments) and authigenic clays. The sandstones in the Gassum-1 well generally have the least ductile fragments and the thinnest red coatings, consequently fracture healing, sutured grain-to-grain contacts and thick quartz overgrowths are more abundant here. Quartz diagenesis is thus dependant on climate-influenced detrital composition and previous diagenetic evolution as well as the burial depth.

Abundant K-feldspar overgrowths form after iron-oxide/hydroxides and thin illitic coatings in the Skagerrak Formation during early burial. K-feldspar is a common authigenic phase in several other continental red beds (Burley, 1984; Burley *et al.*, 1985; Ruffel *et al.*, 2003). This suggests that a high K^+ activity existed in the formation waters during early burial of sediments deposited during arid to semi-arid conditions. High concentrations of silica, K^+, Na^+ and Mg^{2+} characterize the formation waters in climates dominated by low annual precipitation and limited meteoric water flow, accompanied by dissolution of evaporitic minerals and amorphous silica (Bjørlykke & Aagaard, 1992) and in tropical humid climates (Van de Kamp, 2010). The prevalence of authigenic K-feldspar over other minerals could be related to the low temperatures at early burial, where K-feldspar is stable unlike, for example, albite (De Ros *et al.*, 1994; Worden & Burley, 2003; Mark *et al.*, 2005). Preferential albite dissolution accompanied by stable K-feldspar grains in the Skagerrak Formation from the Gannet Field, UK was caused by organic acids generated during maturation of the organic matter in the Kimmeridge Clay Formation

(Purvis, 1994). An alternative explanation is required for the Skagerrak Formation onshore Denmark, as it has very little organic content, shows no sign of hydrocarbons and typically has only limited abundance of reduction spots and reduced areas. The high stability of K-feldspar relative to albite during deep burial could be caused by potassium from *in situ* dissolution of K-rich volcanic rock fragments and/or supplied from external sources via faults down to the underlying Zechstein deposits, as fractures typically occur in sedimentary units overlying salt pillows (Fig. 2B; Fossen, 2016; Harding & Huuse, 2015). An excessive potassium supply could also explain the relatively low temperatures (47 to 68 and >74°C) in the Skagerrak Formation where detrital smectite is gradually transformed, first to randomly and second to orientated mixed-layer smectite/illite, respectively (Weibel, 1999).

The poikilotopic pore-filling dolomite commonly has a radiating extinction thereby resembling saddle dolomite. Saddle dolomite forms at temperatures higher than 60 to 80°C and lower than 90 to 160°C under the influence of pore fluids of higher salinity than sea water (Spötl & Pitman, 1998). This fits with the temperatures (60 to 80°C) calculated from the oxygen isotopic composition of saddle dolomite (Fig. 12). Dolomite was the dominant authigenic carbonate cement during burial and hence indicates that the Mg activity was high and the Fe activity low due to the oxidizing conditions. The calcite cement in deeper buried sandstones (e.g. the Mors-1, Thisted-2 wells) has depleted $\delta^{18}O$ content indicating recrystallization during burial of early formed caliche. The depleted $\delta^{13}C$ values of calcite and dolomite from the Gassum-1 well suggest a local input of carbon from organic material decomposition.

Sediments deposited under humid conditions – Gassum Formation

The stable carbonate cement changed during burial from siderite and calcite to mainly ankerite and occasionally Fe-rich dolomite in the Gassum Formation (Fig. 5). Ankerite occurs as pervasive or patchy poikilotopic and sparry cement commonly with floating detrital grains which suggests ankerite either formed as early diagenetic cement, or by replacement of detrital carbonate grains or fossils and/or early calcite and siderite cement. A late diagenetic origin of the ankerite cement is confirmed by infrequent enclosure of quartz overgrowths in ankerite cement (Fig. 9F) and is supported by its oxygen isotopic composition of $\delta^{18}O_{PDB}$: −14 to −13‰, which corresponds with ankerite precipitation temperatures of 110 to 120°C (according to the fractionation factors by Zeng, 1999). Ankerite dominates the carbonate cements in shoreface and lagoonal sandstones at estimated maximum burial depths >3500 m, which suggest that fossils in the marine environments may have been an important internal source for preceding calcite cement, although mouldic shapes cannot be documented. Furthermore, occasionally preserved calcite cement shows dissolution features prior to enclosure in ankerite cement. All of these features suggest that ankerite cement formed partly at the expense of earlier calcite (and siderite) cement.

The detrital clays in the Gassum Formation are dominated by illite and kaolinite (Fig. 11), as is the intercalated and overlying Fjerritslev Formation (Pedersen, 1982; Schmidt, 1985), which shows that a humid climate promoted precipitation of illite and kaolinite in the sediment source area as well as during diagenesis of the Gassum Formation. Clay coatings in fluvial sandstones may have been dominated by kaolinitic clays at the time of infiltration, although they consist of illite at present burial depth. Illitization of kaolinite at increased burial may have promoted dissolution of K-feldspar in order to supply K^+ for the illite precipitation.

Increasing maximum albite content with increasing burial depth, vacuolized zones in detrital feldspar, albite overgrowths and growth of authigenic albite on the delicate skeletal texture of the original detrital feldspar remnants are evidence of diagenetic albitization and albite precipitation in the deeply buried parts of the Gassum Formation (Figs 5 and 10D). The increase in albite abundance with burial depth of the Gassum Formation suggests a temperature constraint on the process, and previous investigations show that albitization of K-feldspar occurs over a temperature range of 65 to 120°C (Saigal *et al.*, 1988; Aagaard *et al.*, 1990) or 100 to 130°C (Mansurbeg *et al.*, 2008). Aagaard *et al.* (1990) showed that the formation waters from shallow buried North Sea Jurassic sandstones (50 to 80°C) lie in the stability field of K-feldspar, whereas formation waters from deeper burial (>90°C) are stable with respect to albite or at the K-feldspar–albite equilibrium line. The marine influenced pore fluids in the Gassum Formation probably had a high initial sodium content, which could promote albite precipitation. Albite, however, is equally abundant in fluvial and shoreface sandstones in the Gassum Formation. The albite precipitation (overgrowths and albitization of other feldspar types) takes place at deeper burial, at which point the pore fluid composition may have changed due to upwards driven compaction water of higher sodium content possibly expelled from the surrounding shales.

Mass transfer of sodium into the sandstones and potassium out is required to account for the observed albitization (Aagaard *et al.*, 1990; Land & Milliken, 2010). Several possible sources of sodium have been considered: intrastratal evaporites (Saigal *et al.*, 1988; Land & Milliken, 2010), connate water (Saigal *et al.*, 1988) and ion

exchange with neighbouring shales (Boles & Franks, 1979; Aagaard *et al.*, 1990; Thyne, 2001; Steefel *et al.*, 2005). Sodium may have been expelled from the surrounding shales, as Upper Jurassic (Kimmeridgian–Volgian) North Sea clays have been interpreted as mixed-layer illite/smectite consisting of alternating interlayers of K and Na (Hansen & Lindgreen, 1989). Potassium is transported into interbedded shales, thereby promoting illitization of smectite, which liberates Na or Mg, Fe and Si that can be transported from the shales into the sandstones where sodium assists in the albitization of K-feldspar. A similar process could take place in detrital clays internally in the sandstone although volumetrically in sufficient amounts.

The crystal morphology of authigenic quartz is governed by the distribution of illitic coatings. Quartz outgrowth occurs locally in the Gassum Formation where thick illitic coatings cover the detrital grains. Quartz overgrowths cover entire grains and expand into the pore space where illitic coatings are missing or disrupted. Stylolites preferentially occur along concentrations of mica in illite-poor sandstones.

Fluid circulation or transitional climate

In the majority of the basin, the Skagerrak and Gassum formations are separated by impermeable mudstones of the thick Oddesund and/or Vinding formations hindering exchange of pore fluids. As the intervening fine-grained sediments also represent a relatively long time period, deposition of the arid/semi-arid Skagerrak Formation is clearly separated from deposition of the humid Gassum Formation by a considerable period of time during which the climate changed. In contrast, the two formations are in direct contact at the margin of the basin shown by the Vedsted-1 and Flyvbjerg-1 wells (Fig. 3). This provides an opportunity to investigate the diagenetic processes influenced by, and reflecting, a transitional climate zone from the older arid to semi-arid climate to more humid conditions. The sandstones in the uppermost Skagerrak Formation in the Vedsted-1 well are very coarse-grained braided stream deposits that formed along the basin margin contemporaneously with deposition of marine deposits of the Gassum Formation in the central parts of the basin (Bertelsen, 1978, 1980; Nielsen, 2003).

The diagenetic alterations of the Skagerrak Formation as observed in rock samples from the Vedsted-1 well resemble those observed in the Gassum Formation, by having a mineralogically mature composition, abundant kaolinite and ankerite cement and lacking iron-oxide/hydroxide coatings. This reflects sediments deposited in the transitional phase from semi-arid to humid climate. The diagenetic alteration of the uppermost Skagerrak Formation may also have been influenced by abundant diluted and reducing fluids during deposition of the lowermost Gassum Formation thus this part of the Skagerrak Formation experienced leaching and changed formation water composition. The lack of siderite cement in the Skagerrak Formation from the Vedsted-1 core, although common in the Gassum Formation, show that the earliest diagenesis differs slightly from that in the Gassum Formation. In the Flyvbjerg-1 well, the cored interval of the Skagerak Formation is characterized by caliche and reddish mudstone and hence does not appear to be influenced by leaching water or the humid climate.

Reservoir porosity and permeability

Some universal effects on reservoir porosity and permeability can be documented by comparing sandstones deposited under arid to semi-arid with sandstones deposited under humid conditions (Skagerrak and Gassum formations, respectively). Permeability varies with grain size independently of climatic conditions, although most clearly for fluvial and shoreface depositional environments. The highest permeabilities occur in the shallowly buried sandstones of which the maximum values occur in the Gassum Formation. During burial, the influence of the depositional environment (and especially grain size) lessens and the diagenetic path becomes more important. The fluvial sandstones deposited under arid to semi-arid climate have generally higher permeabilities at specific porosities than the fluvial, estuarine-fluvial and shoreface sandstones deposited under the humid climate. The red coatings formed during early diagenesis in the arid to semi-arid sandstones may retard some cement types, especially quartz overgrowths, and thereby preserve more primary porosity during burial than the discontinuous clay coatings in most of the sandstones deposited under humid climate. The exceptions to this general relationship are (i) thick illite coatings formed after red coatings in the Skagerrak Formation from the Thisted-2 core (Fig. 13A) and (ii) continuous chlorite coatings in the Gassum Formation from the Vedsted-1 core (Fig. 13D and E). The continuous chlorite coatings preserve high permeabilities (>400 mD) in sandstones buried down to 2400 m, although siderite cement may hamper this in some cases (Weibel *et al.*, 2017). The higher illite content in the medium-grained sandstones in Thisted-2 core compared with the general trend for medium-grained sandstones of the Skagerrak Formation, including the deeper buried Mors-1 core, results in a lower permeability versus porosity trend (compare the trend for medium-grained sandstones of the Skagerrak Formation with those of the Thisted-2 core in Fig. 13A). The illite precipitation seems to be associated with availability of potassium, either sourced via faults from deeper lying sediments or from dissolution of internal K-rich volcanic rock fragments.

Detrital clays (>10%) reduce permeability to a similar degree as illitic clays (>5%) (Fig. 13B). The fibrous morphology of illitic clays compared with the tangential morphology of detrital clays is responsible for the higher reduction of permeability. Kaolinite (>5%) seems to affect the permeability less than other clay types (Fig. 13).

Pore-filling carbonate (calcite, ankerite and dolomite) cement occurring with abundances >20% results in relatively low porosities and permeabilities, 3 to 9% and 0·04 to 21 mD, respectively (Fig. 13). Siderite cement, an early cement in the Gassum Formation, consists of numerous small crystals, and thereby reduces the permeability more at a specific porosity compared with the other carbonate types and consequently forms the lowermost permeability–porosity trend for the shoreface sandstones (Fig. 13E). The very late ankerite cement in the Gassum Formation mainly affects deeply buried sandstones at a late stage, except the cases where ankerite replaces calcite and siderite cement. Precipitation of pedogene calcite and dolomite results in infilling of porosity at relatively shallow burial depths in the Skagerrak Formation. However, the overall observation is that carbonate cement, when present, seems to decrease porosity and permeability independently of the climate.

The quartz cement may have a framework stabilizing effect, as samples from the Gassum Formation having >10% quartz cement occasionally have relatively high permeabilities (Fig. 13). However, the abundance of other cement types may be equally important.

CONCLUSIONS

Despite the same sediment source area being active during deposition of both the Skagerrak and the Gassum formations, the composition of the detrital material that reached the Norwegian–Danish Basin during Triassic and Jurassic times varied due to differing degrees of alteration under the arid to semi-arid and humid climates, respectively. The alteration intensity was less under the arid to semi-arid climate during deposition of the Skagerrak Formation than under the humid climate of the Gassum Formation. In the shallowly buried parts of the Skagerrak Formation, K-feldspar occurs combined with plagioclase of varying Ca content, whereas K-feldspar dominates the feldspar group in the shallowly buried parts of the Gassum Formation. Rock fragments are more common and the heavy mineral assemblage more diverse in the Skagerrak Formation compared with the Gassum Formation, which is characterized by less common rock fragments and more stable heavy minerals, such as zircon and rutile.

The early diagenetic physiochemical conditions reflect the climate regime (Fig. 14). In the arid to semi-arid climate, low annual precipitation created an overall oxidizing environment, under which iron-oxides/hydroxides were stable. Evaporative processes locally played an important role in precipitation of gypsum and caliche calcite in the Skagerrak Formation. Higher annual precipitation during the humid climate promoted vegetation and caused leaching of feldspar followed by formation of kaolinite. Kaolinite is particularly abundant in the Gassum Formation sandstones, although the intercalated mudstones also generally have a higher kaolinite/illite ratio than the Skagerrak Formation, where illite, mixed-layer illite/smecite and smectite are more common. The abundant organic matter in the Gassum Formation created reducing conditions under which the stable authigenic iron phases were pyrite, Fe-rich chlorite and

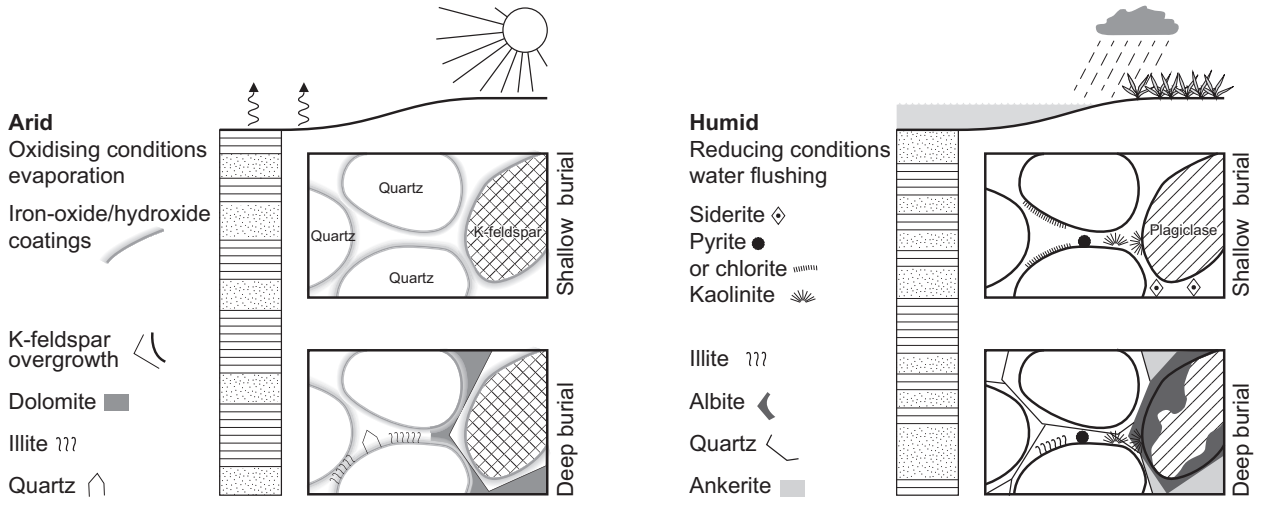

Fig. 14. Graphical overview showing the characteristic diagenetic changes occurring in sandstones deposited under arid to semi-arid and humid climate, respectively.

siderite. The alteration of detrital Fe-Ti oxides is equally sensitive to the redox conditions; therefore, hematite remains unaltered, magnetite is replaced by hematite and ilmenite is gradually replaced by leucoxene under the oxidizing conditions of the Skagerrak Formation. Hematite and magnetite are dissolved and ilmenite intensively altered to leucoxene under the reducing conditions of the Gassum Formation. However, locally, variations in the geochemical conditions may create exceptions from the trends determined by the overall climate. Thus, the diagenesis of reduction spots in the Skagerrak Formation deviates from the general red bed diagenesis and resembles the diagenesis in the sandstones of the Gassum Formation deposited under humid conditions.

The climate defined the early diagenetic regime by controlling the availability of water, the chemistry of the groundwater and the groundwater level. Combined the climatically defined detrital composition and early diagenetic regime subsequently affected the burial diagenesis. Diagenesis of the sandstones deposited in an arid to semi-arid climate can clearly be distinguished from the diagenesis of the sandstones deposited in a humid climate. Continued oxidizing conditions also during burial of the Skagerrak Formation are documented by iron-oxide/hydroxide coatings enclosed in zones of authigenic quartz, dolomite and between authigenic clays (illitic and chloritic clays), whereas iron was incorporated in ankerite cement under the reducing conditions of the Gassum Formation. Authigenic albite mainly formed in the Gassum Formation during increased burial and was associated with sodium supplied during diagenesis of the enveloping marine claystones, which contain mixed-layer clay of low Na-content. Thus, the albite authigenesis is consequently related to the depositional environment rather than the climate conditions.

Authigenic quartz and illite formed in all sandstones during increased burial, and seem to be universal during burial diagenesis, contrary to several other cement types, like ankerite, dolomite, chlorite, etc., which are associated with early diagenesis and hence climate and depositional environments. Quartz cement seems to be more abundant in the Gassum Formation than in the Skagerrak Formation, where the occurrence of quartz outgrowths is more common due to abundant red coatings. Illite mainly formed from kaolinite in the Gassum Formation, but from smectite through mixed-layer illite/smectite in the Skagerrak Formation. Consequently, the diagenetic routes may have been different, but the formed authigenic phases similar.

The reservoir conditions can be explained by the depositional environment, especially the grains size, climatic and palaeohydrological conditions during deposition, burial depth and the diagenetic path during burial. Shallowly buried fluvial, estuarine-fluvial and shoreface sandstones with porosity >20% represent the highest permeabilities. The permeabilities vary according to grain sizes, and the maximum values occur in sandstones deposited under humid conditions. The diagenetic path during burial reflects the climatic and palaeohydrological conditions during deposition in such a way the red coatings in the arid to semi-arid sandstones seem to preserve the primary porosity and permeability to deeper burial than sandstones deposited under humid conditions with discontinuous clay coatings.

ACKNOWLEDGEMENTS

This contribution is published with the permission of the Geological Survey of Denmark and Greenland and is an outcome of the project "The geothermal energy potential in Denmark – reservoir properties, temperature distribution and models for utilisation" under the programme Sustainable Energy and Environment funded by the Danish Agency for Science, Technology and Innovation. Editor in Chief, Peter Swart, and Associate Editor, Adrian Immenhauser, and two anonymous reviewers are thanked for constructive comments, which helped to improve the final manuscript. Special thanks are addressed to the International Association of Sedimentologists for funding of the open access of the paper. Troels Laier is thanked for important information on the pore fluid composition in the Danish subsurface. Gunver Krarup Pedersen helpfully provided clay mineralogical information on the Fjerritslev Formation. Lisbeth Løvig Nielsen and Nanna Rosing-Schow are thanked for plugging and sampling. Hans Jørgen Lorentzen and Marga Jørgensen are thanked for measuring porosity and permeability. Dan Olsen is thanked for performing quality control of the old data set. Thanks also to Jette Halskov for preparation of the drawings.

References

Aagaard, P., Egeberg, P.K., Saigal, G.C., Morad, S. and **Bjørlykke, K.** (1990) Diagenetic albitization of detrital K-feldspars in Jurassic, Lower Cretaceous and Tertiary clastic reservoir rocks from offshore Norway, II. Formation water chemistry and kinetic considerations. *J. Sed. Petrol.*, **60**, 575–581.

Ahlberg, A., Arndorff, L. and **Guy-Ohlson, D.** (2002) Onshore climate change during the Late Triassic marine inundation of the Central European Basin. *Terra Nova*, **14**, 241–248.

American Petroleum Institute (1998) *API RP 40, Recommended Practice for Core Analysis*, 2nd edn. American Petroleum Institute, Washington, DC.

Bensing, J.P., Mozley, P.S. and **Dunbar, N.W.** (2005) Importance of clay in iron transport and sediment

reddening: Evidence from reduction features of the Abo Formation, New Mexico, U.S.A. *J. Sed. Res.*, **75**, 562–571.

Berner, R.A. (1969) Migration of iron and sulfur within anaerobic sediments during early diagenesis. *Am. J. Sci.*, **267**, 19–42.

Bertelsen, F. (1978) The Upper Triassic – Lower Jurassic Vinding and Gassum Formations of the Norwegian-Danish Basin. *Dan. Geol. Unders. Ser. B*, **3**, 26.

Bertelsen, F. (1980) Lithostratigraphy and depositional history of the Danish Triassic. *Dan. Geol. Unders. Ser. B*, **4**, 59.

Besly, B.M., Burley, S.D. and **Turner, P.** (1993) The late Carboniferous "Barren Red Bed" play of the Silver Pit area, Southern North Sea. In: *Petroleum Geology of Northwest Europe: Proceedings of the 4th Conference* (Ed. J.R. Parker), pp. 727–740. The Geological Society, London.

Bjørlykke, K. (1984) Formation of secondary porosity: how important is it? In: *Clastic Diagenesis* (Eds D.A. McDonald and R.C. Surdam), *Am. Assoc. Pet. Geol. Mem.*, **37**, 277–286.

Bjørlykke, K. (1998) Clay mineral diagenesis in sedimentary basins – a key to the prediction of rock properties. Examples from the North Sea Basin. *Clay Miner.*, **33**, 15–34.

Bjørlykke, K. and **Aagaard, P.** (1992) Clay minerals in North Sea sandstones. In: *Origin, Diagenesis and Petrophysics of Clay Minerals in Sandstones* (Eds D.W. Houseknecht and E.D. Pittman), *SEPM Spec. Publ.*, **47**, 243–268.

Bjørlykke, K., Jahren, J., Mondol, N.H., Marcussen, Ø., Croize, D., Peltonen, C. and **Thyberg, B.** (2009) *Sediment Compaction and Rock Properties*. Search and Discovery Article 50192. Poster presentation at AAPG International Conference and Exhibition, Cape Town, South Africa, October 26-29, 2008.

Boles, J.R. and **Franks, S.G.** (1979) Clay diagenesis in Wilcoz sandstones of southwest Texas, implications of smecite diagenesis on sandstone cementation. *J. Sed. Petrol.*, **49**, 55–70.

Burgess, D.T., Kettler, R.M. and **Loope, D.B.** (2016) The geologic context of wonderstone: acomplex, outcrop-scaled pattern of iron-oxide cement. *J. Sed. Res.*, **86**, 498–511.

Burley, S. (1984) Patterns of diagenesis in the Sherwood Sandstone Group (Triassic), United Kingdom. *Clay Mineral.*, **19**, 403–440.

Burley, S.D., Kantorowicz, J.D. and **Waugh, B.** (1985) Clastic diagenesis. *Geol. Soc. London. Spec. Publ.*, **18**, 189–226.

Canfield, D.E., Raiswell, R. and **Bottrell, S.** (1992) The reactivity of sedimentary iron minerals toward sulphide. *Am. J. Sci.*, **292**, 659–683.

Carothers, W.W., Adami, L.H. and **Rosenbauer, R.J.** (1988) Experimental oxygen isotope fractionation between siderite-water and phosphoric acid liberated CO_2-siderite. *Geochim. Cosmochim. Acta*, **52**, 2445–2450.

Cerling, T.E. and **Quade, J.** (1993) Stable carbon and oxygen isotopes in soil carbonates. Climate change in continental isotopic records. *Geophys. Monograph. Am. Geophys. Union*, **78**, 217–231.

Christenson, G.E. and **Purcell, C.** (1985) Correlation and age of Quaternary alluvial fan sequences, Basin and Range province, southwestern United States. *Geol. Soc. Am. Spec. Publ.*, **203**, 115–122.

Coleman, M.L. (1993) Microbial processes: controls on the shape and composition of carbonate concretions. *Mar. Geol.*, **113**, 127–140.

Coleman, M.L. and **Raiswell, R.** (1981) Carbon, oxygen and sulphur isotope variations in concretions from the Upper Lias of N. E. England. *Geochim. Cosmochim. Acta*, **45**, 329–340.

Crowley, T.J. and **North, G.R**. (1991) *Paleoclimatology: Oxford Monographs on Geology and Geophysics No. 16*, Oxford University Press, New York, 339 pp.

Craig, H. (1957) Isotopic standards for carbon and oxygen correction factors for mass spectrometric analysis of carbon dioxide. *Geochim. Cosmochim. Acta*, **12**, 133–149.

Deer, W.A., Howie, R.A. and **Zussmann, J.** (1985) *An Introduction to Rock-Forming Minerals. Fifteenth Impression*, p. 528. Longman Group Limited, Essex, 528 pp.

De Ros, L.F., Sgarbi, G.N.C. and **Morad, S.** (1994) Multiple authigenesis of K-feldspar in sandstones: evidence from the Cretaceous Areado Formation, São Francisco, Central Brazil. *J. Sed. Res.*, **A64**, 778–787.

Deegan, C.E. and **Scull, B.J.** (1977) A standard lithostratigraphic nomenclature for the Central and Northern North Sea. *Inst. Geol. Sci. Norw. Petrol. Direct. Bull.*, **1**, 36.

Dill, H.G. (1998) A review of heavy minerals in clastic sediments with case studies from the alluvial-fan through the nearshore-marine environments. *Earth-Sci. Rev.*, **45**, 103–132.

Dorn, R.I. (2013) The role of climatic change in alluvial fan development. In: *Geomorphology of Desert Environments* (Eds A.D. Abrahams and A. Parson), pp. 723–742. Springer, London.

Dorn, R.I., Deniro, M.J. and **Ajie, H.O.** (1987) Isotopic evidence for climatic influence on alluvial-fan development in Death Valley, California. *Geology*, **15**, 108–110.

El-ghali, M.A.K., Morad, S., Mansurbeg, H., Caja, M.A., Sirat, M. and **Ogle, N.** (2009) Diagenetic alterations related to marine transgression and regression in fluvial and shallow marine sandstones of the Triassic Buntsandstein and Keuper sequence, the Paris Basin, France. *Mar. Pet. Geol.*, **26**, 289–309.

Fisher, Q.J., Knipe, R.J. and **Worden, R.H.** (2000) Microstructures of deformed and non-deformed sandstones from the North Sea: implications for the origins of quartz cement in sandstones. In: *Quartz Cementation in Sandstones* (Eds R. Worden and S. Morad), *Spec. Publ. Int. Assoc. Sedimentol.*, **29**, 129–146.

Folk, R.L. (1966) A review of grain-size parameters. *Sedimentology*, **6**, 73–93.

Fossen, H. (2016) Chapter 20: salt tectonics. In: *Structural Geology*, 2nd edn, pp. 417–439. University of Bergen, Norway.

Francis, J.E. (2009) Palaeoclimates of Pangea – geological evidence. *Can. Soc. Petrol. Geol.*, **17**, 265–274.

Friedman, I. and **O'Neil, J.R.** (1977) Compilation of stable isotopic fractionation factors of geochemical interest. *U.S. Geol. Surv. Prof. Pap.*, **440-KK**, 12.

Friis, H. (1976) Weathering of a Neogene fluviatile fining-upwards sequence at Voervadsbro, Denmark. *Bull. Geol. Soc. Denmark*, **25**, 99–105.

Friis, H. (1978) Heavy minerals variability in Miocene marine sediments in Denmark: a combined effect of weathering and reworking. *Sed. Geol.*, **21**, 169–188.

Friis, H. (1987) Diagenesis of the Gassum Formation Rhaetian-Lower Jurassic, Danish Subbasin. *Geol. Surv. Denmark A*, **18**, 41.

Giles, M.R., Stevenson, S., Martin, S.V., Cannon, S.J.C., Hamilton, P.J., Marshall, J.D. and **Samways, G.M.** (1992) The reservoir properties and diagenesis of the Brent Group: a regional perspective. In: *Geology of the Brent Group* (Eds A.C. Morton, R.S. Haszeldine, M.R. Giles and S. Brown), *Geol. Soc. London. Spec. Publ.*, **61**, 289–327.

Gluyas, J.G., Robinson, A.G., Emery, D., Grant, S.M. and **Oxtoby, N.H.** (1993) The link between petroleum emplacement and sandstone cementation. In: *Petroleum Geology of North-West Europe: Proceedings of the Fourth Conference* (Ed. J.R. Parker), *Geol. Soc. London*, 1395–1402.

Griffiths, J., Worden, R.H., Wooldridge, L., Duller, B. and **Utley, J.** (2015) *Predicting Clay Mineralogy Distribution in Deeply Buried Sandstone Reservoirs Using a Modern Estuarine Analogue Approach*. 31st International Association of Sedimentologists Meeting, Krakow (Abstract).

Hamberg, L. (1994) *Anatomy of Clastic Coastal Sequences in the Rhaetian Gassum Formation, Stenlille, Denmark*. Unpublished PhD Thesis. University of Copenhagen, Denmark, 90 pp.

Hamberg, L. and **Nielsen, L.H**. (2000) Shingled, sharp-based shoreface sandstones: depositional response to stepwise forced regression in a shallow basin, Upper Triassic Gassum Formation, Denmark. In: *Sedimentary Responses to Forced Regressions* (Eds D. Hunt and R.L. Gawthorpe), *Geological Society Special Publications (London)* **172**, 69–89.

Hansen, P.L. and **Lindgreen, H.** (1989) Mixed-layer illite/smectite diagenesis in Upper Jurasic claystones from the North Sea and onshore Denmark. *Clay Miner.*, **24**, 197–213.

Harding, R. and **Huuse, M.** (2015) Salt on the move: multi stage evolution of salt diapirs in the Netherlands North Sea. *Mar. Pet. Geol.*, **61**, 39–55.

Hillier, S. (1994) Pore-lining chlorites in siliciclastic reservoir sandstones: electron microprobe SEM and XRD data, and implications for their origin. *Clay Miner.*, **29**, 665–679.

Hillier, S. (2003) Quantitative analysis of clay and other minerals in sandstones by X-ray powder diffraction (XRPD). *Int. Assoc. Sedimentol. Spec. Publ.*, **34**, 213–251.

Horibe, Y. and **Oba, T.** (1972) Temperatures scales of aragonite–water and calcite–water systems. *Fossils*, **23**24, 69–70.

Ixer, R.A., Turner, P. and **Waugh, B.** (1979) Authigenic iron and titanium oxides in Triassic red beds: (St. Bees Sandstone), Cumbria, Northern England. *Geol. J.*, **14**, 179–192.

Japsen, P. and **Bidstrup, T.** (1999) Quantification of late Cenozoic erosion in Denmark based on sonic data and basin modelling. *Bull. Geol. Soc. Denmark*, **46**, 79–99.

Japsen, P., Green, P.F., Nielsen, L.H., Rasmussen, E.S. and **Bidstrup, T.** (2007) Mesozoic-Cenozoic exhumation events in the eastern North Sea Basin: a multi-disciplinary study based on palaeothermal, palaeoburial, stratigraphic and seismic data. *Basin Res.*, **19**, 451–490.

Jeans, C.V., Mitchell, J.G., Fisher, M.J., Wray, D.S. and **Hall, I.R.** (2001) Age, origin and climatic signal of English Mesozoic clays based on K/Ar signatures. *Clay Miner.*, **36**, 515–539.

Kazerouni, A.M., Poulsen, M.L., Friis, H., Svendsen, J.B. and **Hansen, J.V.** (2013) Illite/smectite transformation in detrital glaucony during burial diagenesis of sandstone: a study from Siri Canyon – Danish North Sea. *Sedimentology*, **60**, 679–692.

Ketzer, J.M., Morad, S., Nystuen, J.P. and **De Ros, L.F.** (2003) The role of the Cimmerian unconformity (Early Cretaceous) on the kaolinitization and reservoir quality evolution of Triassic sandstones of the Snorre Field, North Sea. In: *Clay-Mineral Cementation in Sandstones* (Eds R. Worden and S. Morad), *Int. Assoc. Sedimentol. Spec. Publ.*, **34**, 353–374.

Keulen, N.T., Frei, D., Riisager, P. and **Knudsen, C.** (2012) Analysis of heavy minerals in sediments by computer-controlled scanning electron microscopy (CCSEM): principles and applications. Quantitative Mineralogy and Microanalysis of Sediments and Sedimentary Rocks. *Mineral. Assoc. Canada Short Course*, **42**, 167–184.

Kutzbach, J.E. and **Gallimore, R.G.** (1989) Pangaean climates: megamonsoons of the Megacontinent. *J. Geophys. Res.*, **94**, 3341–3357.

Land, L.S. and **Milliken, K.L.** (2010) Feldspar diagenesis in the Frio Formation, Brazoria Country, Texas Gulf Coast. *Geology*, **9**, 31–318.

Larsen, G. (1966) Rhaetic-Jurassic-Lower Cretaceous sediments in the Danish Embayment. (A heavy-mineral study). *Geol. Surv. Denmark II Ser.*, **91**, 127.

Larsen, G. and **Friis, H.** (1975) Triassic heavy-mineral associations in Denmark. *Geol. Surv. Denmark Yearbook*, **1974**, 33–47.

Liboriussen, J., Ashton, P. and **Tygesen, T.** (1987) The tectonic evolution of the Fennoscandian Border Zone in Denmark. *Techtonophysics*, **137**, 21–29.

Longiaru, S. (1987) Visual comparators for estimating the degree of sorting from plane and thin sections. *J. Sed. Res.*, **57**, 791–794.

Manspeizer, W. (1994) The break-up of Pangea and its impact on climate: consequences of Variscan-Alleghanide orogenic collapse. In: *Pangea: Paleoclimate, Tectonics and Sedimentation During Accretion. Zenith and Breakup of a Supercontinent* (Ed. G.D. Klain), *Geol. Soc. Am. Spec. Publ. Pap.*, **288**, 169–185.

Mansurbeg, H., Morad, S., Salem, A., Marfil, R., El-ghali, M.A.K., Nystuen, J.P., Caja, M.A., Amorosi, A., Garcia, D. and **La Iglesia, A.** (2008) Diagenesis and reservoir quality evolution of palaeocene deep-water, marine sandstones, the Shetland-Faroes Basin, British continental shelf. *Mar. Pet. Geol.*, **25**, 514–543.

Mark, D.F., Parnell, J., Kelly, S.P., Lee, M., Sherlock, S.C. and **Carr, A.** (2005) Dating of multistage fluid flow in sandstones. *Science*, **309**, 2048–2051.

McBride, E.F. (1963) A classification of common sandstones. *J Sediment Res*, **33**, 664–669.

Michelsen, O. (1997) Mesozoic and Cenozoic stratigraphy and structural development of the Sorgenfrei-Tornquist Zone. *Z. Deut. Geol. Ges.*, **148**, 33–50.

Michelsen, O. and **Clausen, O.R.** (2002) Detailed stratigraphic subdivision and regional correlation of the southern Danish Triassic succession. *Mar. Pet. Geol.*, **19**, 563–587.

Mogensen, T.E. (1996) Triassic and Jurassic structural development along the Tornquist Zone, Denmark. *Techtonophysics*, **252**, 197–220.

Mora, G.I., Sheldon, B.T., Elliott, W.C. and **Driese, S.G.** (1998) An oxygen isotope study of illite and calcite in three Appalachian Paleozoic vertic paleosols. *J. Sed. Res.*, **68**, 456–464.

Morton, A.C. (1984) Stability of detrital heavy minerals in Tertiary sandstones of the North Sea Basin. *Clay Miner.*, **19**, 287–308.

Morton, A.C. (1986) Dissolution of apatite in North Sea Jurassic sandstones: implications for the generation of secondary porosity. *Clay Miner.*, **21**, 711–733.

Morton, A.C. and **Hallsworth, C.R.** (1999) Processes controlling the composition of heavy mineral assemblages in sandstones. *Sed. Geol.*, **124**, 3–29.

Mücke, A. (1994) Part I. Postdiagenetic ferruginization of sedimentary rocks (sandstones, oolitic ironstones, kaolins and bauxites) – including a comparative study of the reddening of red beds. In: *Diagenesis, IV* (Eds K.H. Wolf and G.V. Chilingarian), *Dev. Sedimentol.*, **51**, 361–395. Elsevier, Amsterdam.

Nielsen, L.H. (1995) *Genetic Stratigraphy of Upper Triassic – Middle Jurassic Deposits of the Danish Basin and Fennoscandian Border Zone*. Unpublished PhD Thesis. University of Copenhagen, Denmark, 162 pp.

Nielsen, L.H. (2003) Late Triassic-Jurassic development of the Danish Basin and the Fennoscandian Border Zone, southern Scandinavia. In: *The Jurassic of Denmark and Greenland* (Eds J.R. Ineson and F. Surlyk), *Geol. Surv. Denmark Greenland Bull.*, **1**, 459–526.

Nielsen, L.H. and **Japsen, P.** (1991) Deep wells in Denmark 1935–1990: lithostratigraphic subdivision. *Dan. Geol. Unders. Ser. A*, **31**, 179.

Odin, G.S. (1985) Significance of green particles (glaucony, berthierine, chlorite) in arenites. In: *Provenance of Arenites, NATO ASI Series* (Ed. G.G. Zuffa), pp. 279–307. Springer, Netherlands.

Olivarius, M. (2015) *Diagenesis and Provenance of Mesozoic Sandstone Reservoirs Onshore Denmark*. PhD Thesis. Danmarks og Grønlands Geologiske Undersøgelse Rapport 2015/19, 146 pp.

Olivarius, M. and **Nielsen, L.H.** (2016) Triassic paleogeography of the greater eastern Norwegian-Danish Basin: constraints from provenance analysis of the Skagerrak Formation. *Mar. Pet. Geol.*, **69**, 168–182.

Olsen, H. (1988) Sandy braidplan deposits from the Triassic Skagerrak Formation in the Thisted-2 well, Denmark. *Geol. Surv. Denmark Ser. B*, **11**, 26.

Parrish, J.T. (1993) Climate of the Supercontinent Pangea. *J. Geol.*, **101**, 215–233.

Parrish, J.T., Demko, T.M. and **Tanck, G.S.** (1993) Sedimentary palaeoclimatic indicators: what they are and what they tell us. *Phil. Trans. Roy. Soc. London*, **344**, 21–25.

Pedersen, G.K. (1982) *Depositional Environment of a Lowe Jurassic Marine Mudstone Sequence*. Abstract for the IAS 3rd European Regional Meeting 1982, Copenhagen Denmark, pp. 57–59.

Pedersen, P.K. (1998) *Sequence Stratigraphic Analysis of Non-Marine to Marginal Marine Danish Triassic, Supplemented by a Field Study of the Alluvial Architecture of the Ericson Sandstone (USA)*. PhD Thesis. University of Aarhus, Denmark, 18 pp (and appendixes).

Pedersen, G.K. and **Andersen, P.R.** (1980) Depositional environments, diagenetic history and source areas of some Bunter Sandstones in northern Jutland. *Geol. Surv. Denmark Yearbook*, **1979**, 69–93.

Purvis, K. (1994) Extensive dissolution in Triassic reservoir sandstones from the Gannet field, UK North Sea. *Mar. Pet. Geol.*, **11**, 624–630.

Quade, J., Garzione, C. and **Eiler, J.** (2007) Paleoelevation reconstruction using pedogenic carbonates. *Rev. Mineral. Geochem. Mineral. Soc. Am.*, **66**, 1–36.

Rosenbaum, J.M. and **Sheppard, S.M.F.** (1986) An isotopic study of siderites, dolomites and ankerites at high temperatures. *Geochim. Cosmochim. Acta*, **50**, 1147–1150.

Ruffel, A.H., Worden, R.H. and **Evans, R.** (2003) Palaeoclimate controls on spectral gamma-ray radiation from sandstones. *Int. Assoc. Sedimentol. Spec. Publ.*, **34**, 93–108.

Saigal, G.C., Morad, S., Bjørlykke, K., Egeberg, P.K. and **Aagaard, P.** (1988) Diagenetic albitization of detrital K-

feldspar in Jurassic-Lower Cretaceous, and Tertiary clastic reservoir rocks from offshore Norway, I. Textures and origin. *J. Sed. Petrol.*, **58**, 1003–1013.

Schmidt, B.J. (1985) Clay mineral investigation of the Rhaetic – Jurassic – Lower Cretaceous sediments of the Børglum 1 and Uglev 1 wells Denmark. *Bull. Geol. Soc. Denmark*, **34**, 97–110.

Spötl, C. and **Pitman, J.K.** (1998) Saddle (Baroque) Dolomite in Carbonates and Sandstones: a Reappraisal of a Burial-Diagenetic Concept. In: *Carbonate Cementation in Sandstones: Distribution Patterns and Geochemical Evolution* (Ed. S. Morad), pp. 437–460. Blackwell Publishing Ltd., Oxford, UK.

Steefel, C.I., DePaola, D.J. and **Lichtner, P.C.** (2005) Reactive modelling: an essential tool and a new research approach for the Earth sciences. *Earth Planet. Sci. Lett.*, **240**, 539–558.

Storvoll, V., Bjørlykke, K., Karlsen, D. and **Saigal, G.** (2002) Porosity preservation in reservoir sandstones due to grain-coating illite: a study of the Jurassic Garn Formation from the Kristin and Lavrans fields, offshore Mid-Norway. *Mar. Pet. Geol.*, **19**, 767–781.

Surdam, R.C., Jiao, Z.S. and **MacGowan, D.B.** (1993) Redox reactions involving hydrocarbons and mineral oxidants: a mechanism for signigicant porosity enhancement in sandstones. *Am. Assoc. Petrol. Geol.*, **77**, 1509–1518.

Thomsen, E., Damtoft, K. and **Andersen, C.** (1987) Hydrocarbon plays in Denmark outside the Central Trough. In: *Petroleum Geology of North West Europe*, (Eds J. Brooks and K. Glennie), pp. 375–388. Graham and Trotman, London.

Thyne, G. (2001) A model for diagenetic mass transfer between adjacent sandstone and shale. *Mar. Pet. Geol.*, **18**, 743–755.

Van de Kamp, P.C. (2010) Arkose, subarkose, quartz sand, and associated muds derived from felsic plutonic rock in glacial to tropical humid climates. *J. Sed. Res.*, **80**, 895–918.

Van Houten, F.B. (1961) Climatic significance of red beds. In: *Descriptive Palaeoclimatology* (Ed. A.E.M. Nairn), pp. 89–139. Interscience Publishers Inc., New York.

Veevers, J.J. (1994) Pangea: evolution of a supercontinent and its concequences or Earth's paleoclimate and sedimentary environments. In: *Pangea: Paleoclimate, Tectonics and Sedimentation During Accretion. Zenith and Breakup of a Supercontinent* (Ed. G.D. Klain), *Geol. Soc. Am. Spec. Publ. Pap.*, **288**, 13–24.

Vejbæk, O.V. (1997) Dybe strukturer i danske sedimentære bassiner. *Geol. Tidsskr.*, **4**, 1–31.

Walderhaug, O. (1990) A fluid inclusion study of sandstones offshore mid-Norway – possible evidence for continued quartz cementation during oil emplacement. *J. Sed. Petrol.*, **60**, 203–210.

Weibel, R. (1998) Diagenesis in oxidising and locally reducing conditions – an example from the Triassic Skagerrak Formation, Denmark. *Sed. Geol.*, **121**, 259–276.

Weibel, R. (1999) Effects of burial on the clay mineral assemblages in the Triassic Skagerrak Formation, Denmark. *Clay Miner.*, **34**, 619–635.

Weibel, R. and **Friis, H.** (2004) Opaque minerals as keys for distinguishing oxidising and reducing diagenetic conditions in the Lower Triassic Bunter Sandstone, North German Basin. *Sed. Geol.*, **169**, 129–149.

Weibel, R. and **Friis, H.** (2007) Alteration of opaque heavy minerals as reflection of geochemical conditions in depositional and diagenetic environments. In: *Heavy Minerals in Use* (Eds M.A. Mange and D.T. Wright), *Dev. Sedimentol.*, **58**, 277–303. Elsevier.

Weibel, R. and **Groberty, B.** (1999) Pseudomorphous transformation of geothite needles into hematite in sediments of the Triassic Skagerrak Formation, Denmark. *Clay Miner.*, **34**, 657–661.

Weibel, R., Friis, H., Kazerouni, A.M., Svendsen, J.B., Stokkendahl, J. and **Poulsen, M.L.** (2010) Development of early diagenetic silica and quartz morphologies – examples from the Siri Canyon, Danish North Sea. *Sed. Geol.*, **228**, 151–170.

Weibel, R., Lindström, S., Pedersen, G.K., Johansson, L., Dybkjær, K., Whitehouse, M., Boyce, A. and **Leng, M.J.** (2016) Groundwater fluctuations recorded in zonation of microbial siderites from end-Triassic strata. *Sed. Geol.*, **342**, 47–65.

Weibel, R., Olivarius, M., Kristensen, L., Friis, H., Hjuler, M.L., Kjøller, C., Mathiesen, A. and **Nielsen, L.H.** (2017) Predicting permeability of low enthalpy geothermal reservoirs: a case study from the Upper Triassic–Lower Jurassic Gassum Formation, Norwegian–Danish Basin. *Geothermics*, **65**, 135–157.

Wentworth, C.K. (1922) A scale of grade and class terms for clastic sediments. *J. Geol.*, **5**, 377–392.

Worden, H. and **Burley, S.D.** (2003) Sandstone diagenesis: the evolution of sands to stone. In: *Sandstone Diagenesis: Recent and Ancient. Reprint series 4 of the International Association of Sedimentologists* (Eds S.D. Burley and R.H. Worden), pp. 3–44. Blackwell Publishing Ltd, Malden, USA.

Wright, V.P. (1990) A micromorphological classification of fossil and recent calcitic and petrocalcic microstructures. In: *Soil Micromorphology: A Basic and Applied Science* (Ed. L.A. Douglas), *Dev. Soil Sci.*, **19**, 40–407. Elsevier, Amsterdam.

Zeck, H.P., Andriessen, P.A.M., Hansen, K. and **Jensen, P.K.** (1988) Paleozoic paleo-cover of the southern part of the Fennoscandian Shield – fission track constraints. *Tectonophysics*, **149**, 61–66.

Zeng, Y.-F. (1999) Oxygen isotope fractionation in carbonate and sulfate minerals. *Geochem. J.*, **33**, 109–126.

Ziegler, P.A. (1990) *Geological Atlas of Western and Central Europe*, 2nd edn. Shell International Petroleum, Maatschappij.

